ORIGINAL RESEARCH

Epithelial Regeneration After Gastric Ulceration Causes Prolonged Cell-Type Alterations

Eitaro Aihara,[1,*] Andrea L. Matthis,[1,*] Rebekah A. Karns,[2] Kristen A. Engevik,[1] Peihua Jiang,[3] Jiang Wang,[4] Bruce R. Yacyshyn,[5] and Marshall H. Montrose[1]

[1]Department of Molecular and Cellular Physiology, [4]Department of Pathology and Lab Medicine, [5]Division of Digestive Disease, Department of Internal Medicine, University of Cincinnati, Cincinnati, Ohio; [2]Division of Biomedical Informatics, Cincinnati Children's Hospital Medical Center, Cincinnati, Ohio; [3]Monell Chemical Senses Center, Philadelphia, Pennsylvania

SUMMARY

This study shows that prominent histologic, structural, and gene expression abnormalities are observed in macroscopically healed gastric epithelium. Results suggest that the site of ulcer healing is the site of ulcer recurrence and a potential source of further disease.

BACKGROUND & AIMS: The peptic ulcer heals through a complex process, although the ulcer relapse often occurs several years later after healing. Our hypothesis is that even after visual evidence of healing of gastric ulceration, the regenerated epithelium is aberrant for an extended interval, increasing susceptibility of the regenerated epithelium to damage and further diseases.

METHODS: Gastric ulcers were induced in mice by serosal topical application of acetic acid.

RESULTS: Gastric ulcers induced by acetic acid visually healed within 30 days. However, regenerated epithelial architecture was poor. The gene profile of regenerated tissue was abnormal, indicating increased stem/progenitor cells, deficient differentiated gastric cell types, and deranged cell homeostasis. Despite up-regulation of PDX1 in the regenerated epithelium, no mature antral cell type was observed. Four months after healing, the regenerated epithelium lacks parietal cells, trefoil factor 2 (TFF2) and (sex-determining region Y)-box 9 (SOX9) remain up-regulated deep in the gastric gland, and the Na/H exchanger 2 (a TFF2 effector in gastric healing) remains down-regulated. Gastric ulcer healing was strongly delayed in TFF2 knockout mice, and re-epithelialization was accompanied with mucous metaplasia. After *Helicobacter pylori* inoculum 30 days after ulceration, we observed that the gastric ulcer selectively relapses at the same site where it originally was induced. Follow-up evaluation at 8 months showed that the relapsed ulcer was not healed in *H pylori*–infected tissues.

CONCLUSIONS: These findings show that this macroscopically regenerated epithelium has prolonged abnormal cell distribution and is differentially susceptible to subsequent damage by *H pylori*. (*Cell Mol Gastroenterol Hepatol 2016;2:625–647; http://dx.doi.org/10.1016/j.jcmgh.2016.05.005*)

Keywords: Gastric Ulcer Healing; Metaplasia; *H pylori*; SOX9; TFF2; NHE2.

Gastric ulcers, excavations that extend from the epithelial lining to the muscle layer of the stomach, heal through a dynamic process that seeks to restore normal architecture and function to a site of deep tissue erosion. Depending on the size of the erosion, it can take days or months for healing to occur. The mechanisms underlying ulcer healing are not fully understood, although the beneficial effects of *Helicobacter pylori* eradication or inhibition of acid secretion are well established[1–3] to accelerate macroscopic healing of the epithelium over an ulcer bed. Many investigators have focused on ulcer healing by observing the closure of the ulcer hole in short-term (<14 days) animal models of experimental ulceration (or endoscopically in human beings), and developing drugs to accelerate this macroscopic healing process in the preclinical models.[1,2]

Follow-up endoscopy is a common clinical practice. Assessment of gastric ulcer healing usually is based on a visual examination by endoscopy, and not typically on microscopic assessment of mucosal healing.[3] Several long-term follow-up studies have shown a correlation between a history of ulcer and subsequent cancer development.[4–7] Interestingly, the risk of gastric cancer development in ulcer patients with successful *H pylori* eradication has been reported to be reduced by only one third or less compared with eradication failure patients.[4,5,8,9] These results raise the hypothesis that residual abnormalities in the regenerated epithelium after ulcer healing could increase the risk of subsequent damage or disease.
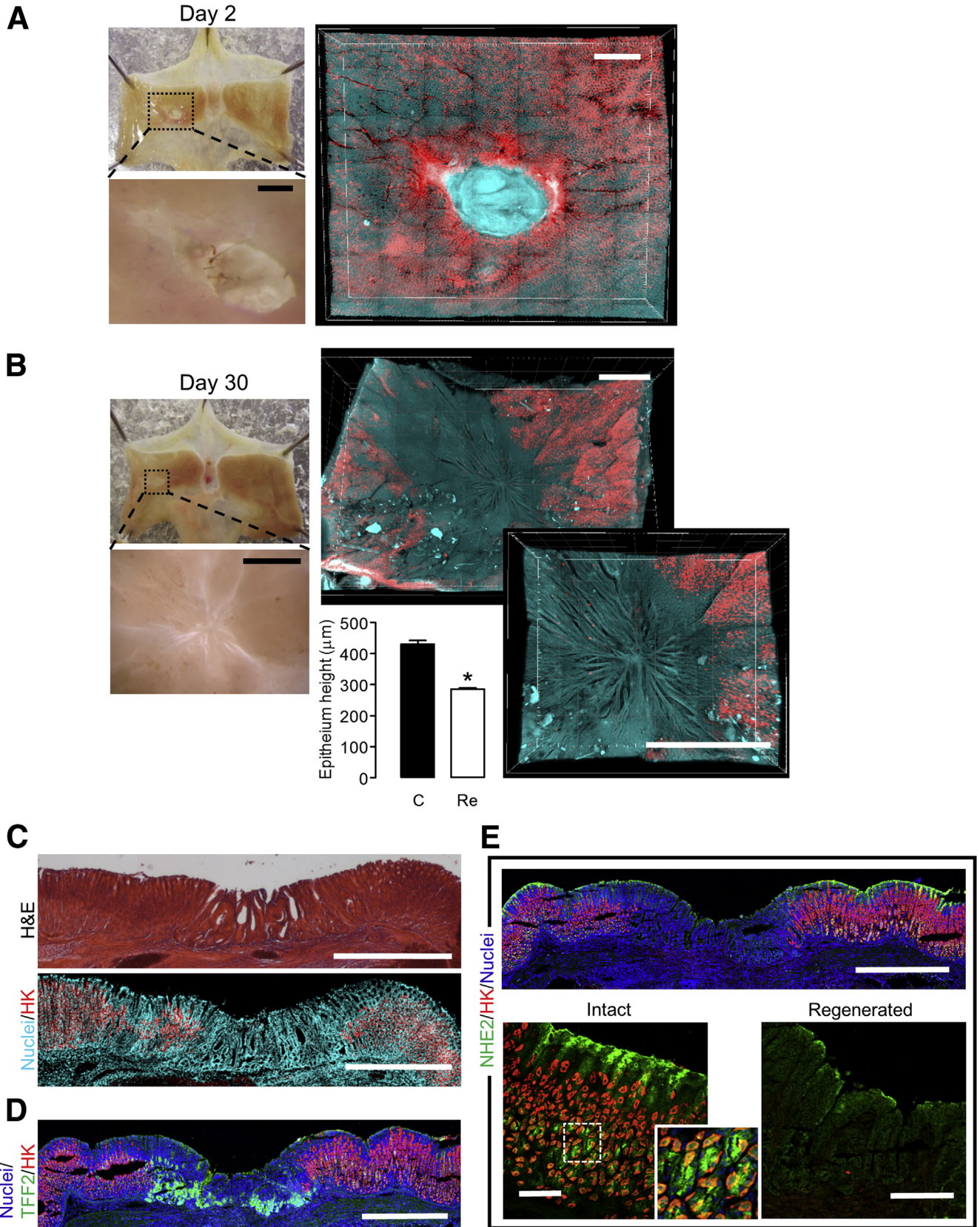
Most current article

Figure 2. Gastric regenerated epithelium morphology at day 30. Gastric tissue was evaluated 30 days after ulcer induction. Gross appearance and (A) 3-dimensional (3D) image of regenerated epithelium stained with nuclei (Hoechst33342: *green*), and (B) 2-dimensional (2D) z-stack image. (C) Side view of 3D constricted image from regenerated epithelium indicated as *white dotted rectangle* in panel A.

Recent studies in rodents observed prominent histologic and structural abnormalities in visually healed tissue at least 28 weeks after ulcer induction, including poor differentiation and/or degenerative changes in glandular cells, increased connective tissue, and disorganized microvascular arrays.[1,3,10] Moreover, in the gastric glands of healed ulcer tissue an up-regulation of trefoil factor 2 (TFF2) and mucin (MUC)6 is accompanied by a lack of parietal cells,[11,12] similar to the metaplastic state identified as a precursor of gastric cancer.[12–14] Interestingly, mice with genetic disruption of the Na/H exchanger isoform sodium hydrogen exchanger 2 (NHE2) have atrophied parietal cells with up-regulation of TFF2,[15,16] and it has been shown that NHE2 is a downstream mediator of TFF2 for the gastric repair of damage.[16] Thus, it is unclear whether regenerated epithelium fully returns to normal, and both TFF2 and NHE2 have been implicated as important elements of gastric epithelial homeostasis.

***

Figure 1. (*See previous page*). **Gastric regenerated epithelium in an acetic acid–induced ulcer mouse model.** Gastric tissue was evaluated (A) 2 days or (B) 30 days after ulcer induction. Gross morphology with low resolution, high resolution of *dotted rectangle* on low-resolution image, and whole mount staining with HK-ATPase (*red*) and nuclei (Hoechst33342: *cyan*). Epithelium height was measured in an uninjured area (C, control) and a regenerated area (Re). *Significant difference at $P < .05$ vs control. Sections of gastric regenerated epithelium at experimental day 30 after ulceration. Images show (C) H&E staining, staining for HK-ATPase (HK: *red*) and cell nuclei (*cyan*), (D) H,K-ATPase (HK: *red*), and TFF2, or (E) NHE2 (*green, bottom panel*: high magnification of intact and regenerated epithelium, *scale bar*: 100 μm), nuclei (*blue*). *Scale bar*: 1 mm.
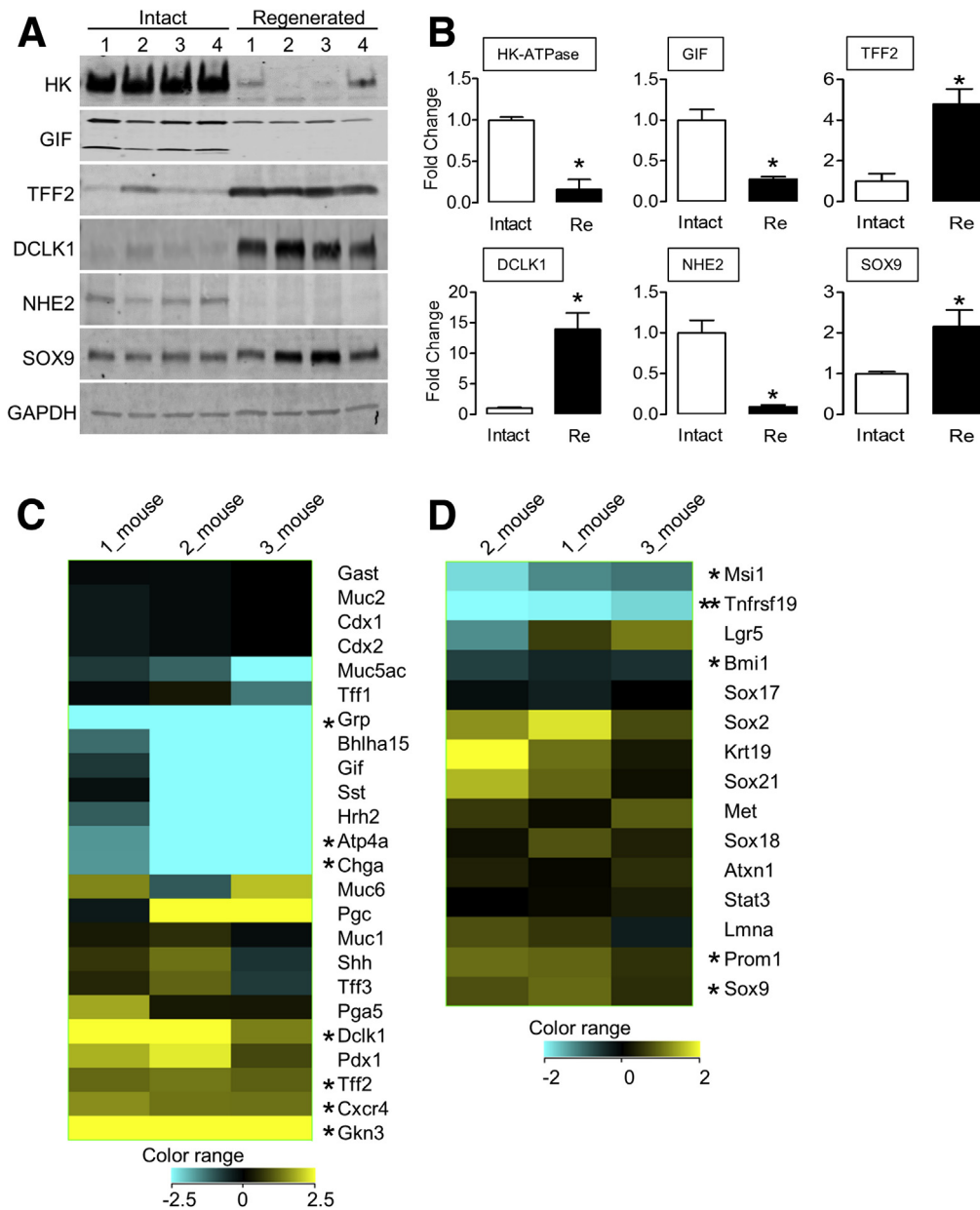
Figure 3. Gastric marker expression in regenerated epithelium. Gastric intact epithelium and regenerated epithelium were isolated 30 days after ulcer induction. (A) Data show Western blot images of HK-ATPase (HK), GIF, TFF2, DCLK1, NHE2, SOX9, or GAPDH as indicated. (B) Compiled analysis of Western blots as in panel A, with results normalized to GAPDH. Results are presented as fold changes to intact epithelium, means ± SEM (N = 4). *Significant difference at $P < .05$ vs intact. Re, regenerated epithelium. Heat map of RNA expression of organ-specific markers, including (C) small intestine, gastric corpus, and gastric antrum, or (D) stem cell markers, in the ulcer regenerated epithelium. Data are represented as log$_2$-transformed gene expression levels in the regenerated epithelium in comparison with the uninjured epithelium from the same mouse stomach (N = 3). *$P < .05$, **$P < .005$ vs uninjured tissue.

The markers of gastric corpus epithelial stem/progenitor cells are largely unknown. The leucine-rich repeat-containing G protein-coupled receptor 5 (Lgr5)+ cell now is recognized as a stem cell in the antrum, small intestine, and colon.[17] However, it is unlikely that Lgr5+ is present in gastric corpus epithelial stem cells.[18] It has been reported that Lgr5+ cells are not involved in developing metaplasia in the corpus in mice, whereas antral-type glands, based on the composition of mucus, are observed in corpus regenerated tissue.[19] Currently, *Troy*-positive cells are identified as quiescent stem-like cells that are expressed in the corpus gland base in a subset of differentiated chief cells, however, there is no active proliferation in the base of the gland in intact tissue.[12,20] In addition, SOX2 is expressed in cells within the gastric adult stem/progenitor compartments and SOX2-positive cells have shown a capacity for self-renewal and differentiation in the gastric corpus.[21] In contrast, SOX9 is widely recognized as a stem/progenitor marker in several tissues, and it has been reported that SOX9 is expressed weakly in the neck/isthmus of the mouse and human gastric corpus region, whereas SOX9 is up-regulated in abnormal gastric epithelium.[22–24]

In the present study, we explored regenerated epithelium morphology and gene profile at 30 days after ulceration, which was visually healed. In addition, we asked if gastric regenerated tissue returns to normal gastric epithelial appearance during a long-term period. Moreover, we asked if the site of regenerated tissue has greater susceptibility to damage, and we investigated the effect of *H pylori* on ulcer regenerated epithelium.

Materials and Methods

Animal Husbandry and Surgery

Experiments used C57BL/6J mice (Jackson Lab, Bar Harbor, ME), in-house bred TFF2 knockout (KO) mice (backcrossed onto a C57BL/6J background until >90% of genomic microsatellite markers were from C57BL/6J), and in-house bred NHE2 (*Slc9A2*) KO mice (FVB/NJ background). Animals were fed a standard rodent chow diet and had free access to water. All mice experiments were conducted according to both Animal Welfare Act Regulations and the Public Health Service Policy on Humane Care and Use of Laboratory Animals. Mice were maintained in an Association for Assessment and Accreditation of Laboratory Animal Care-approved facility and all animal studies followed protocol 04-03-08-01, which was approved by the Institutional Animal Care and Use Committee of the University of Cincinnati.

Gastric ulcers were produced by acetic acid, according to a previously described method with slight modifications.[1] In brief, under isoflurane anesthesia, the abdomen was incised and the intact stomach was exposed. A microcapillary tube (0.7 mm in diameter; Drummond Scientific, Co, Broomall, PA) filled with acetic acid (99%) was placed in contact with the exterior surface of the stomach corpus region and left in place for 25 seconds. Buprenorphine hydrochloride (0.1 mg/kg intraperitoneal Buprenex; Rechkitt Benckiser Pharmaceuticals, Inc, Richmond, VA) was given as pre-emptive analgesia. After the acid was removed, the treated exterior of the stomach was wiped with gauze, the abdomen was closed, and the animals were maintained routinely with food and water. By using this procedure, no incision was made to the stomach as part of the ulcer induction.

To examine ulcer healing, animals were killed at 9 days, 30 days, 44 days, 4 months, or 8 months after ulceration, and the stomach was removed and opened along the greater curvature. The ulcer-induced area was found by serosal observation of white discolored muscle tissue. The area (mm^2) of ulceration on the mucosal side was measured by a digital caliper (Mitutoyo, Kanagawa, Japan). In some cases, *H pylori* was gavaged at day 30 after the ulceration. Control uninfected animals received Brucella broth vehicle (BD Diagnostic Systems, Franklin Lakes, NJ).

Preparation of H pylori

As we described previously,[11] *H pylori* Sydney strain 1 were grown on Columbia blood agar plates (Remel, Lenexa, KS) containing 5% defibrinated horse blood (Colorado Serum, Denver, CO), 0.2% β-cyclodextrin (Sigma, St. Louis, MO), 50 μg/mL cyclohexamide (Sigma), 5 μg/mL vancomycin (Sigma), and 10 μg/mL trimethoprim (Sigma) for 4 days. Bacteria harvested from the plate were grown in Brucella broth (BD Diagnostic Systems) supplemented with 10% fetal bovine serum and a CO_2 gas pack (BD Diagnostic Systems) in a humidified microaerophilic chamber (BBL Gas System with CampyPak Plus packs; BD Microbiology, Sparks, MD) in an incubator at 37°C for 16–18 hours without shaking. Bacteria were collected by centrifuge at 2000 rpm for 5 minutes, and resuspended in Brucella broth without serum. *H pylori* were diluted in 50% glycerol (1:100 dilution) and counted in a hemocytometer. Each mouse received 200 μL Brucella broth containing 10^6 *H pylori* bacteria. Control mice (uninfected group) received 200 μL of Brucella broth alone.

### Quantification of H pylori Levels in Mouse Stomach Tissue

The wet weight was measured for the mouse gastric tissue collected from intact and ulcerated tissue. Tissue was homogenized by Tissue Tearor (model 985370-395; Bio-Spec Products, Bartlesville, OK) in 1 mL saline and 1:10 dilutions were spread on a Columbia blood agar plate containing 5% defibrinated horse blood, 50 μg/mL cyclohexamide, 5 μg/mL vancomycin, and 10 μg/mL trimethoprim. Plates were incubated for 5 days at 37°C in a humidified microaerophilic chamber with a CO_2 gas pack. Colonies were counted and data were normalized using the tissue weight and expressed in colony forming units per gram of tissue.

Quantitative Real-Time Polymerase Chain Reaction

Total RNA was isolated from either the intact or regenerated epithelium of the stomach using TRI Reagent (Molecular Research Center, Inc, Cincinnati, OH) and single-stranded cDNA was synthesized by the iScript cDNA synthesis kit (Bio-Rad, Hercules, CA). Quantitative real-time polymerase chain reaction (PCR) was performed using the SYBR Green PCR Master Mix (Applied Biosystems, Foster, CA) with the following specific primers: hydrogen potassium exchanger adenosine triphosphatase (HK-ATPase) (forward: 5'-AGATGGTGTTTGCTCGAACC-3' and reverse: 5'-TCCAGCAA-GATCATGTCAGC-3'), TFF2 (forward: 5'-GCAGTGCTTT-GATCTTGGATGC-3′ and reverse: 5'-TCAGGTTGGAAAAGC AGCAGTT-3'), NHE2 (forward: 5′-CTTCTGATTCGGGAAAACA-3′ and reverse: 5'-ATCAGGATCTCCTTGGCTTG-3'), SOX9 (forward: 5'-CGGAACAGACTCACATCTCTCC-3 and reverse: '5'-GCTTGCACGTCGGTTTTGG-3'), or glyceraldehyde-3-phosphate dehydrogenase (GAPDH) (forward: 5'-AAC-GACCCCTTCATTGAC-3' and reverse: 5'-TCCACGACA-TACTCAGCAC-3'). Each PCR amplification was performed in duplicate wells in a StepOnePlus Real-Time PCR System (Applied Biosystems).

Immunofluorescence

Mouse intact or regenerated stomach tissue was embedded in optimal cutting temperature compound (Sakura Finetek, Inc, Torrance, CA), frozen, and stored at -80°C. Serial cryosections (10 μm) were prepared by cryostat. The section was stained with H&E. For immunostaining, sections were fixed with 4% paraformaldehyde, followed by heat-activated antigen retrieval (Vector Laboratories, Burlingame, CA), and then incubated with goat serum (5%) or 3% bovine serum albumin for 60 minutes. Sections then were incubated with primary antibodies indicated later for 60 minutes at room temperature. Primary antibodies to the H^+/K^+-ATPase α subunit (mouse
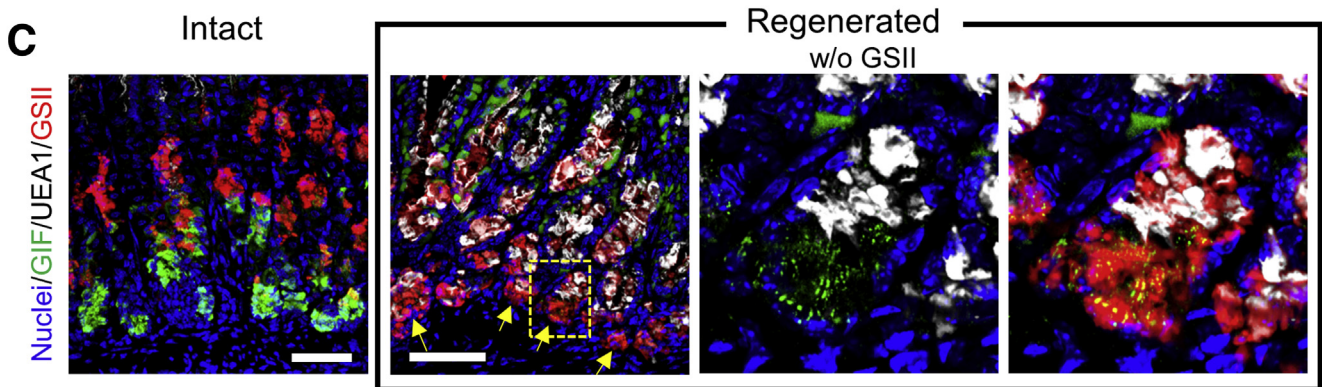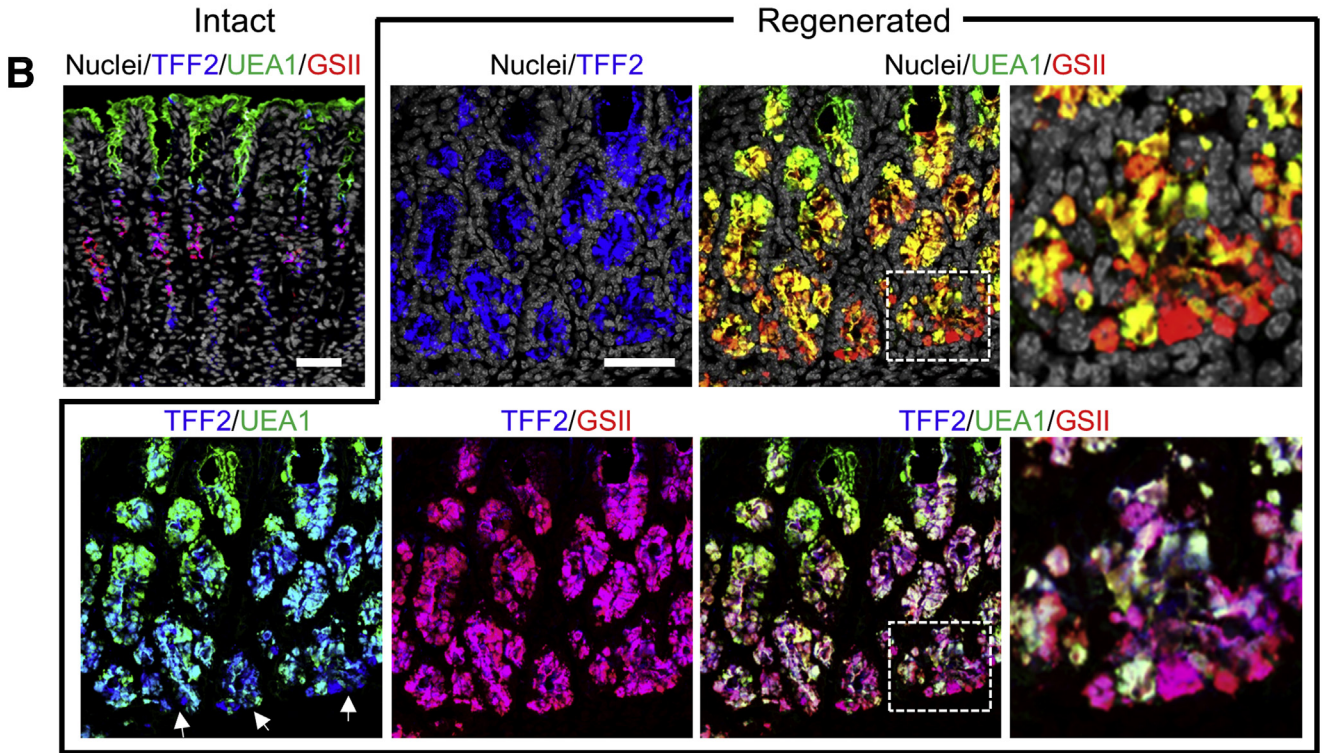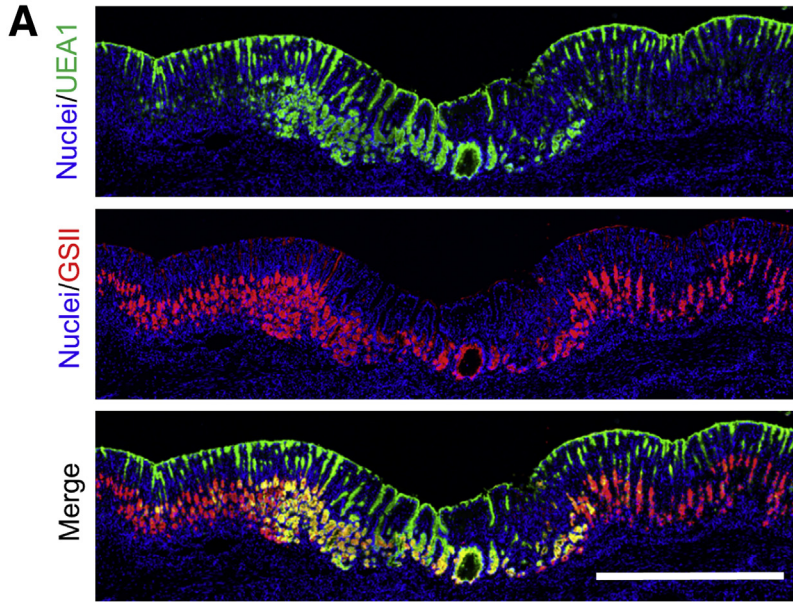
monoclonal, 1:1000; Thermo Fisher Scientific, Inc, Waltham, MA; or rabbit polyclonal, 1:1000; Santa Cruz, Biotechnology, Inc, Dallas, TX), TFF2 (rabbit polyclonal, 1:200), gastric intrinsic factor (GIF) (rabbit polyclonal, 1:100; Abcam, Cambridge, MA), doublecortin-like kinase 1 (DCLK1) (mouse monoclonal, 1:200, or rabbit polyclonal 1:1000; Abcam), SOX9 (rabbit polyclonal, 1:1000; EMD Millipore, Billerica, MA), NHE2 (rabbit polyclonal, 1:200), Ki67 (rabbit polyclonal, 1:200; Abcam), pancreatic and duodenal homeobox 1 (PDX1) (goat polyclonal, 1:5000; Abcam), gastrin (rabbit polyclonal, 1:500; Dako, Carpinteria, CA), or SOX2 (mouse monoclonal, 1:200; Abcam) were used. Secondary antibodies (Alexa 633–labeled goat anti-mouse IgGγ1, 1:1000; Alexa 488–labeled goat anti-rabbit IgG, 1:1000; 1:500 for H$^+$/K$^+$-ATPase, TFF2, GIF, DCLK1, SOX9, NHE2, Ki67, or SOX2; Alexa 633–labeled goat anti-rabbit IgG for gastrin; Alexa 647–labeled donkey anti-rabbit IgG 1:1000 for SOX9 and Alexa 488–labeled donkey anti-goat IgG 1:1000 for PDX1) were incubated for 60 minutes at room temperature. In some cases, Alexa 647–lectin GSII (1:100; Life Technologies, Carlsbad, CA) and rhodamine–UEA-1 (1:100; Vector Laboratories) were incubated for 60 minutes at room temperature. Nuclear staining was performed by incubation with Hoechst 33342 (Invitrogen, Carlsbad, CA) at 1 μg/mL for 30 seconds. Sections were imaged with Zeiss LSM710 confocal microscopy (Carl Zeiss, Oberkochen, Germany).

Whole Mount Staining

Mouse intact or regenerated stomach tissues were fixed with 4% paraformaldehyde overnight at 4°C, followed by Dent's fixative (80% methanol + 20% dimethylsulfoxide) for 2 hours. After rehydration, tissues were incubated with goat serum (4%) for 2 hours. Tissues then were incubated with primary antibody to the H$^+$/K$^+$-ATPase α subunit (rabbit polyclonal, 1:100; Santa Cruz) overnight at 4°C, followed by secondary antibodies (Alexa 633–labeled goat anti-rabbit IgG, 1:400; Invitrogen), which were incubated overnight at 4°C. Nuclear staining was performed by incubation with Hoechst 33342 (Invitrogen) at 10 μg/mL for 60 minutes. The tissue then was dehydrated with methanol and a clearing agent was applied (2:1, benzyl benzoate:benzyl alcohol). Whole-mount images were obtained via z-stack using the Zeiss LSM710, and 3-dimensional images were rendered by Imaris 7.7 (Bitplane, Zurich, Switzerland).

Western Blot Analysis

Extracted proteins from mouse intact or regenerated stomach tissues were separated on a 1%–15% gradient sodium dodecyl sulfate–polyacrylamide gel electrophoresis (Bio-Rad), and transferred to a polyvinylidene difluoride membrane (Immobilon-P; EMD Millipore). Membranes were incubated for 1 hour with Odyssey blocking buffer (Li-Cor Biosciences, Lincoln, NE), and then incubated with primary antibodies to H$^+$/K$^+$-ATPase α subunit (mouse monoclonal, 1:10,000), GIF (rabbit polyclonal, 1:1000), TFF2 (rabbit polyclonal, 1:1000), DCLK1 (rabbit polyclonal, 1:2000), NHE2 (rabbit polyclonal, 1:1000), SOX9 (rabbit polyclonal, 1:2000), or GAPDH (mouse monoclonal 1:10,000). Membranes then were washed and incubated for 1 hour in goat anti-rabbit secondary antibody (Alexa Fluor 680, 1:1000 dilution; Invitrogen) or goat anti-mouse secondary antibody (IR800 dye, 1:10,000; Li-Cor Biosciences). Fluorescent blots were imaged and quantified using an Odyssey infrared imaging system (Li-Cor Biosciences). Immunoreactive bands were quantified using background-corrected integrated pixel intensity. Results were normalized to GAPDH, then shown as fold change to value from intact tissue or wild-type (WT) tissue.

RNA Sequence and Analysis

Stomach corpus regenerated tissue and corpus noninvolved tissue were harvested after 30 days of ulceration under a dissection scope. Tissue was homogenized in TRI Reagent. Extracted total RNA was purified by the PureLink DNA Mini Kit (Life Technologies), followed by quantification with a Qubit Fluorometer (Life Technologies). The messenger RNA (mRNA) was poly-A selected and converted into a single-stranded cDNA library for Next Generation Sequencing using the Illumina HiSeq 2500 (Illumina, Inc, San Diego, CA) rapid sequencing system at the Cincinnati Children's Hospital Medical Center Sequencing Core. RNA sequencing (RNAseq) was single-end 75–base pair reads with an average read depth of 30 million per sample. All analyses were performed in GeneSpring 12.6 (Agilent Technologies, Santa Clara, CA) after removal of barcodes and primers.

Sequence data were aligned to the mouse reference genome (mm10), with reference annotations produced by the University of California, Santa Cruz.[25] Reads with multiple mappings were removed, and aligned reads subsequently were filtered on quality, including a quality threshold of 30 or greater, and zero N values allowed. Reads per kilobase per million reads were computed using quantified read counts for each sample, subsequently normalized using the DESeq algorithm and thresholded to 1. Normalized counts were baselined to the median of control samples. The expression data are available through NCBI Gene Expression Omnibus (GSE76565).

Statistical Analysis

All values are reported from representative experiments as the means ± SEM from multiple experiments. All results

---

Figure 4. (*See previous page*). **Mucous metaplasia in regenerated epithelium.** Immunofluorescence was performed 30 days after acetic acid application. (*A*) Representative images show UEA-1 (*green*), GSII (*red*), and nuclei (Hoechst33342: *blue*). *Scale bar*: 1 mm. (*B*) Representative images show TFF2 (*blue*), UEA-1 (*green*), GSII (*red*), and nuclei (*white*) in the intact and regenerated epithelium. *White arrows* in TFF2 and UEA-1 indicate cells that are TFF2 positive but UEA-1 negative. *Scale bar*: 50 μm. (*C*) Representative images show GIF (*green*), UEA-1 (*white*), GSII (*red*), and nuclei (*blue*) in the intact and regenerated epithelium. *Yellow arrows* indicate cells that are GIF positive in the regenerated epithelium. *Scale bar*: 50 μm.
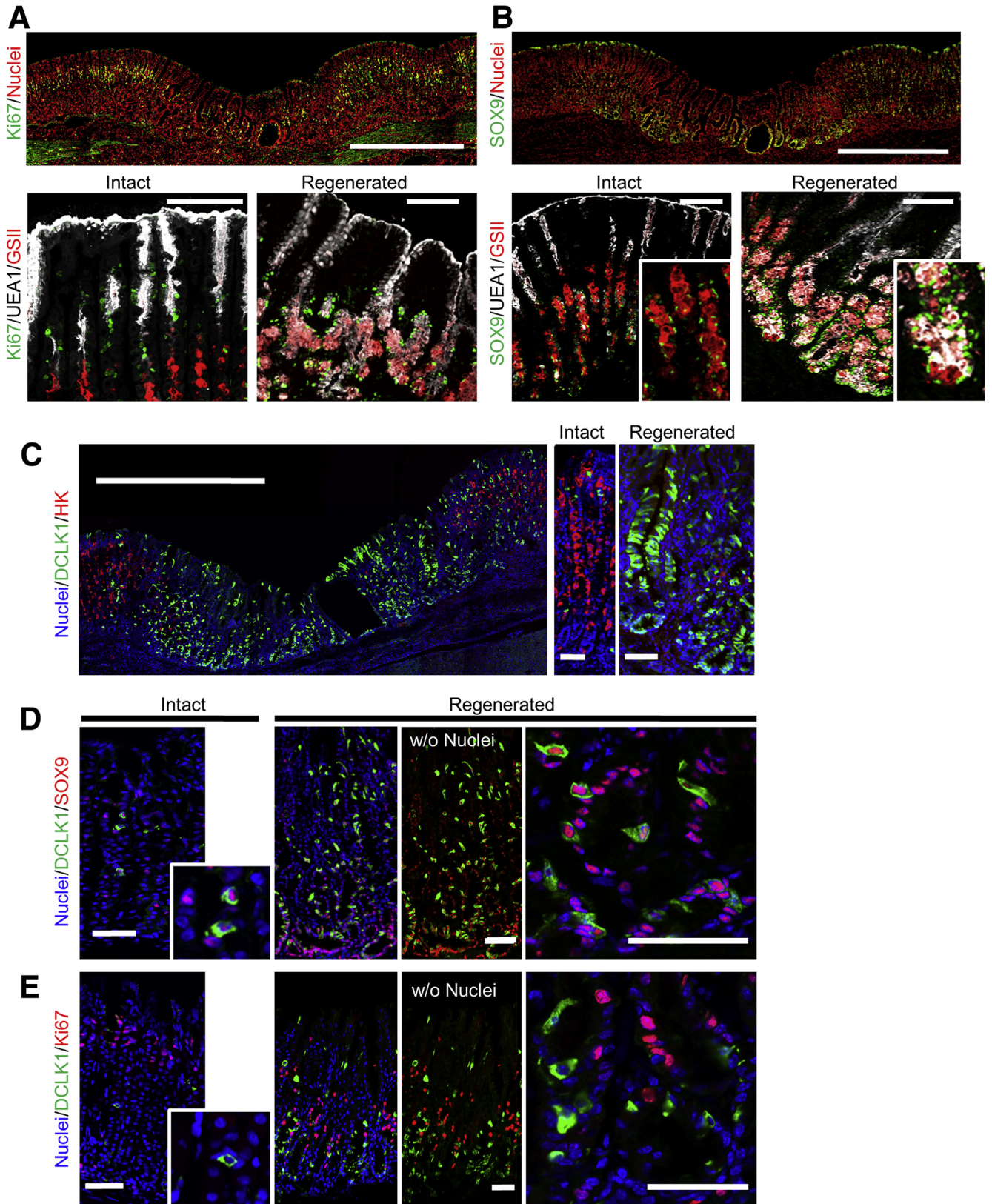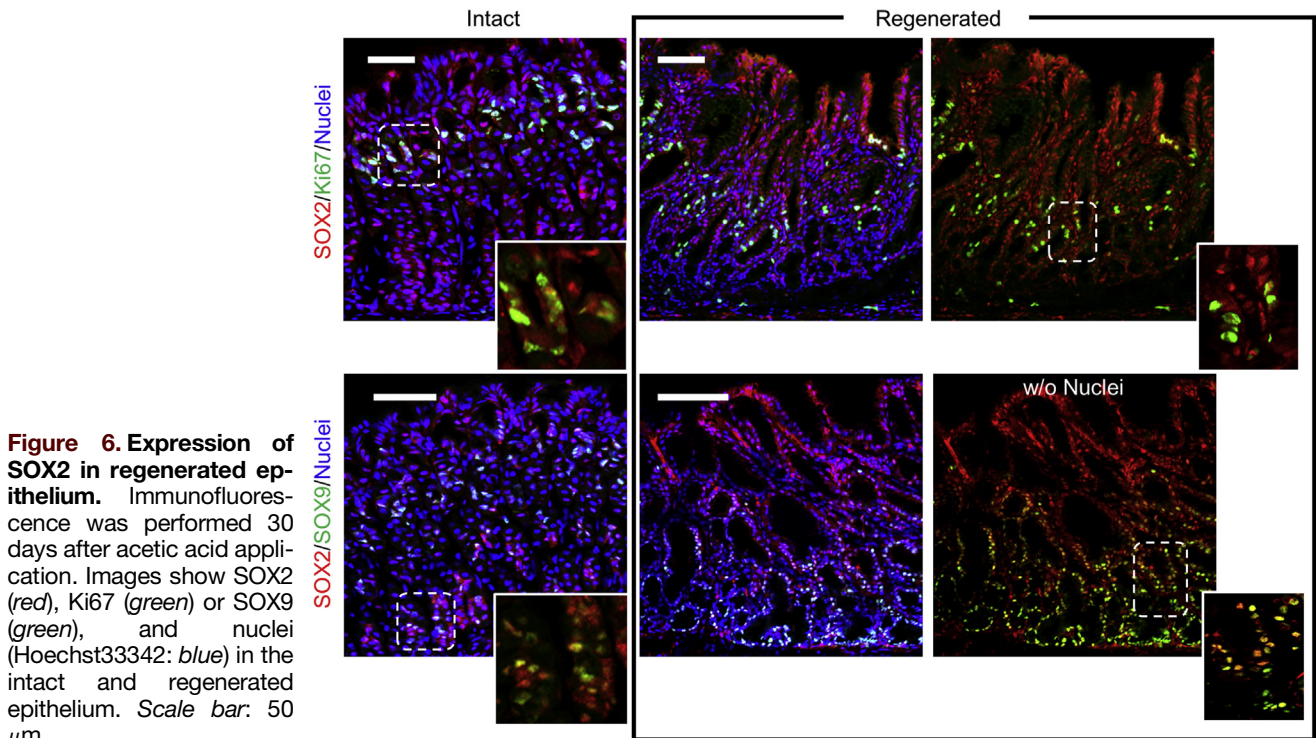
Figure 6. Expression of SOX2 in regenerated epithelium. Immunofluorescence was performed 30 days after acetic acid application. Images show SOX2 (*red*), Ki67 (*green*) or SOX9 (*green*), and nuclei (Hoechst33342: *blue*) in the intact and regenerated epithelium. *Scale bar*: 50 μm.

were reproduced in at least 3 animals. Statistical significance was determined using an unpaired Student t test, or 1-way analysis of variance with the Dunnett multiple comparison post hoc test. A P value less than .05 was considered significant.

Expression values were compared between regenerated and noninvolved tissue from the same mouse stomach using paired tests, with significance defined as a P value less than .05 and a fold change magnitude greater than 1.5 (n = 1165 significant genes) (Supplementary Table 1). In addition, genes with known involvement in gastric function were assessed for significance and fold change between regenerated and noninvolved tissues. Heat maps were generated and clustered on both gene and condition, using the Euclidean distance metric and average linkage rule. Ontologic analyses and biological networking were performed using GATACA (https://gataca.cchmc. org), ToppGene Suite (https://toppgene.cchmc.org),[26] ToppCluster (https://toppcluster.cchmc.org),[27] and Cytoscape3.[28]

All authors had access to the study data and reviewed and approved the final manuscript.

Results

Regenerated Epithelial Appearance and Gene Expression

Acetic acid–induced ulcers are a well-established rodent model that has similar features of human ulcers.[1] Consistent with our previous observation,[11] serosal application of acetic acid induced necrosis of the local gastric epithelium, covering the ulcerated area with dead cells. It is noted that no HK-ATPase–positive cells were found in the ulcerated area, whereas HK-ATPase–positive cells (bright red) with bright Hoechst nuclear staining (indication of cell death) were seen on the edge of the ulcerated area undergoing cell death at day 2 (Figure 1*A*). At day 30, the ulcerated area was visually covered by newly generated epithelium, although microscopic observation showed the regenerated epithelial appearance to be distinguished from normal gastric epithelium, lacking HK-ATPase–positive cells (Figure 1*B*). Characteristically, the regenerated surface epithelium was connected to many glandular infoldings (Figure 2 and Supplementary Movie 1). Sectioned gastric regenerated tissue lacked HK-ATPase–positive cells (Figure 1*C*), and had

---

Figure 5. (*See previous page*). Proliferation zone and stem cells in the gastric regenerated epithelium. Gastric tissue was evaluated 30 days after ulcer induction. Sections of gastric regenerated epithelium were stained with (*A*) Ki67 and (*B*) SOX9. *Top*: Ki67 or SOX9 (*green*) and nuclei (Hoechst33342: *red*). *Scale bar*: 1 mm. In contrast, *bottom*: high magnification of Ki67 or SOX9 (*green*) co-stained with UEA-1 (*white*) and GSII (*red*) in the intact and regenerated epithelium. *Scale bar*: 100 μm. Sections of regenerated gastric epithelium were co-stained with (*C*) DCLK1 and HK-ATPase, (*D*) SOX9, or (*E*) Ki67. (*C*) Images show DCLK1 (*green*), HK-ATPase (HK: *red*), and nuclei (*blue*) in low magnification (*left panel*: scale bar: 1 mm) and high magnification of intact and regenerated epithelium (*right panel*: scale bar: 50 μm). Double staining for (*D*) DCLK (*green*) and SOX9 (*red*) or (*E*) Ki67 (*red*), and nuclei (*blue*) in the intact and regenerated epithelium. *Scale bar*: 50 μm.
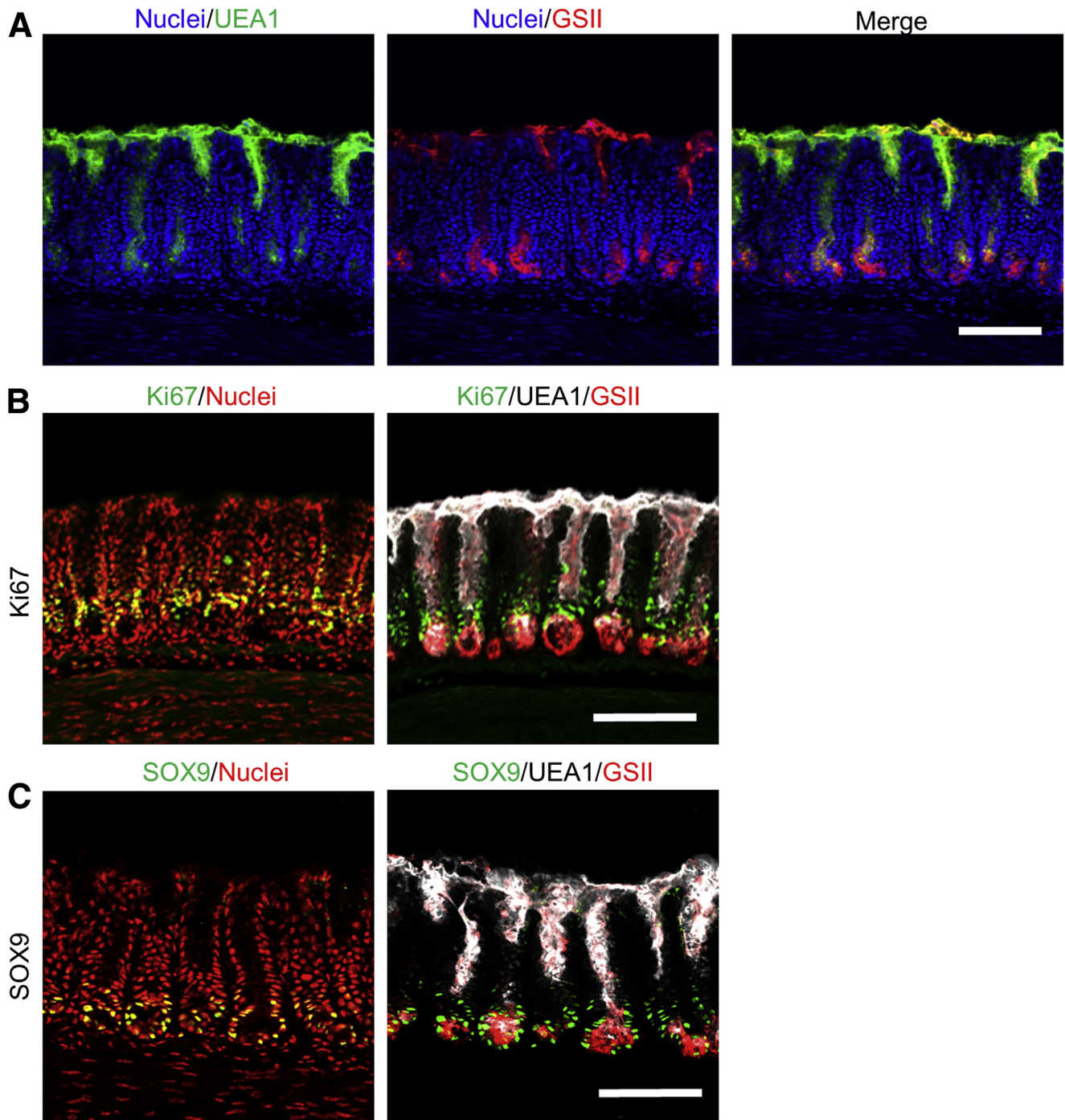
Figure 7. Expression of UEA-1, GSII, Ki67, and SOX9 in the gastric antrum. (*A*) Sections of gastric antrum were stained with UEA-1 (*green*), GSII (*red*), and nuclei (Hoechst33342: *blue*). *Scale bar*: 100 μm. (*B* and *C*) *Left*: Ki67 or SOX9 (*green*) and nuclei (*red*), respectively; *right*: Ki67 or SOX9 (*green*) co-stained with UEA-1 (*white*) and GSII (*red*) in the sections of gastric antrum, respectively. *Scale bar*: 100 μm.

significantly reduced mucosal thickness vs normal epithelium (Figure 1*B*). Consistent with our previous finding,[11] we observed up-regulation of TFF2 in the ulcer margin as well as at the base of regenerated epithelium where HK-ATPase–positive cells were lacking (Figure 1*D*). The changes in TFF2 and HK-ATPase were confirmed independently by Western blot (Figure 3*A* and *B*) and RNAseq (Figure 3*C*). RNAseq also showed up-regulation of C-X-C chemokine receptor type 4 (CXCR4), a putative TFF2 receptor,[16,29] in the regenerated epithelium (Figure 3*C*). Interestingly, we observed down-regulation of NHE2 in the regenerated tissue (Figures 1*E* and 3*A* and *B*). The RNAseq data reported that the gastric surface marker, Muc5ac, and the parietal cell marker, HK-ATPase (Atp4a), H2 receptor (Hrh2), endocrine cell marker, and chromogranin A (Chga) were down-regulated (Figure 3*C*). In addition to down-regulation of
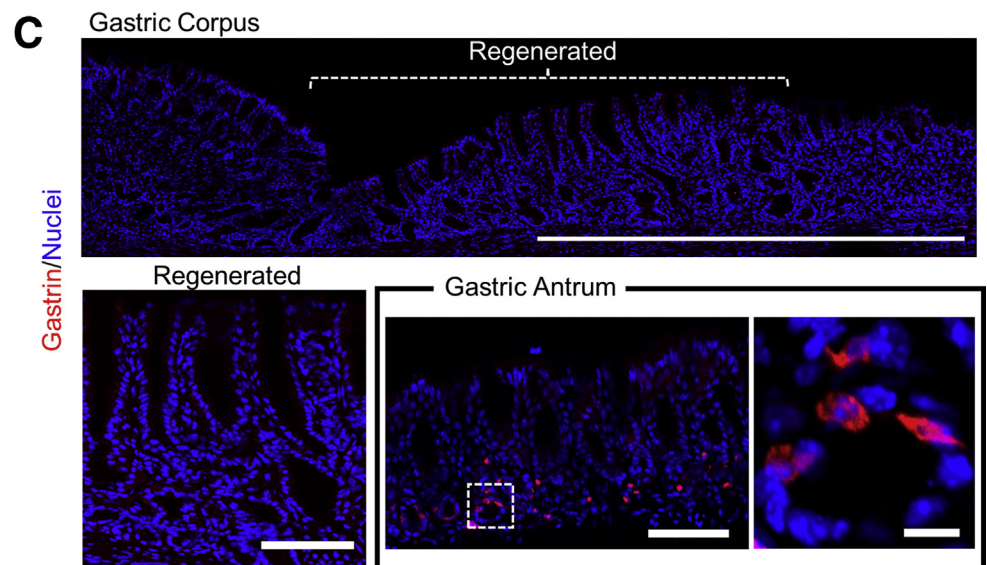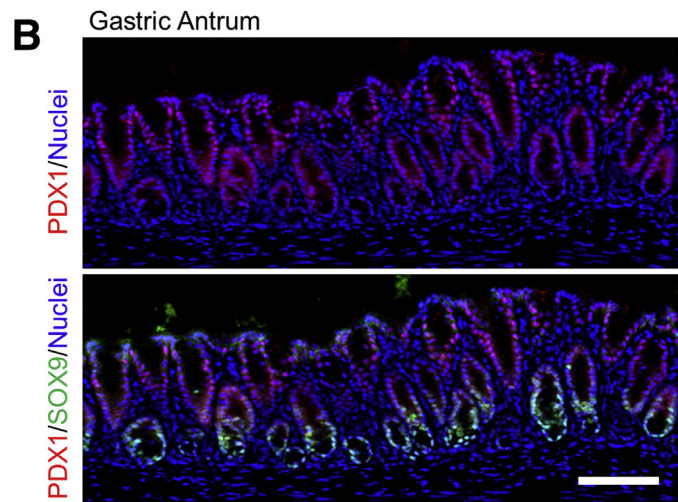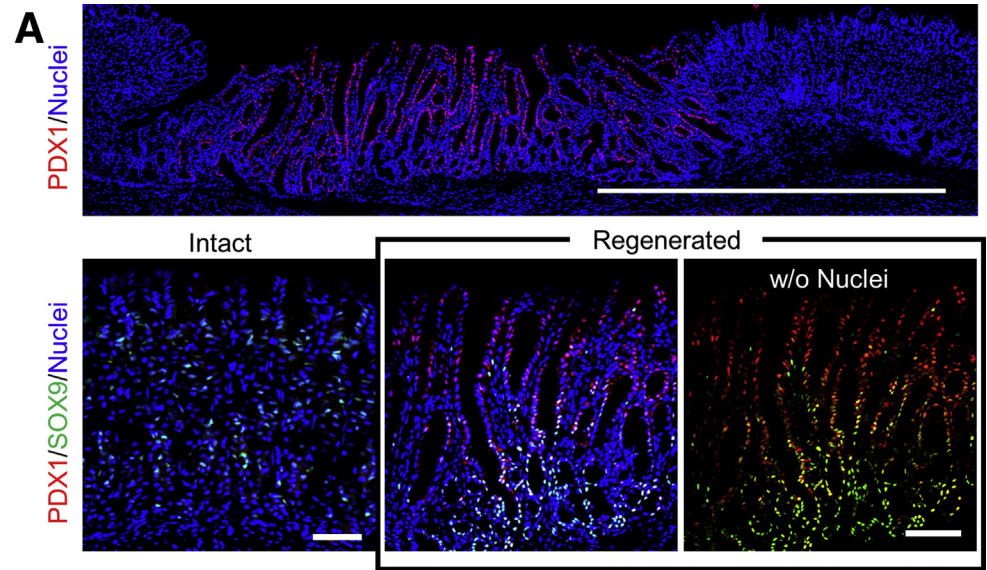
Figure 8. Expression of PDX1 in regenerated epithelium. Immunofluorescence was performed 30 days after acetic acid application. (*A*) *Upper*: PDX1 (*red*) and nuclei (Hoechst33342: *blue*). *Scale bar*: 1 mm. *Lower*: high magnification of PDX1 (*red*) co-stained with SOX9 (*green*) and nuclei (*blue*) in the intact and regenerated epithelium. *Scale bar*: 50 μm. (*B*) PDX1 (*red*) with SOX9 (*green*) and nuclei (*blue*) in gastric antrum. *Scale bar*: 100 μm. (*C*) Low (*upper panel*: *scale bar*: 1 mm) or high (*lower panel*: *scale bar*: 100 μm) magnification of gastrin (*red*) and nuclei (*blue*) staining in the regenerated epithelium. In addition, images show low (*scale bar*: 100 μm) or high (from *dotted rectangle* on low-resolution image, *scale bar*: 10 μm) resolution of gastrin (*red*) and nuclei (*blue*) expression in gastric antrum.
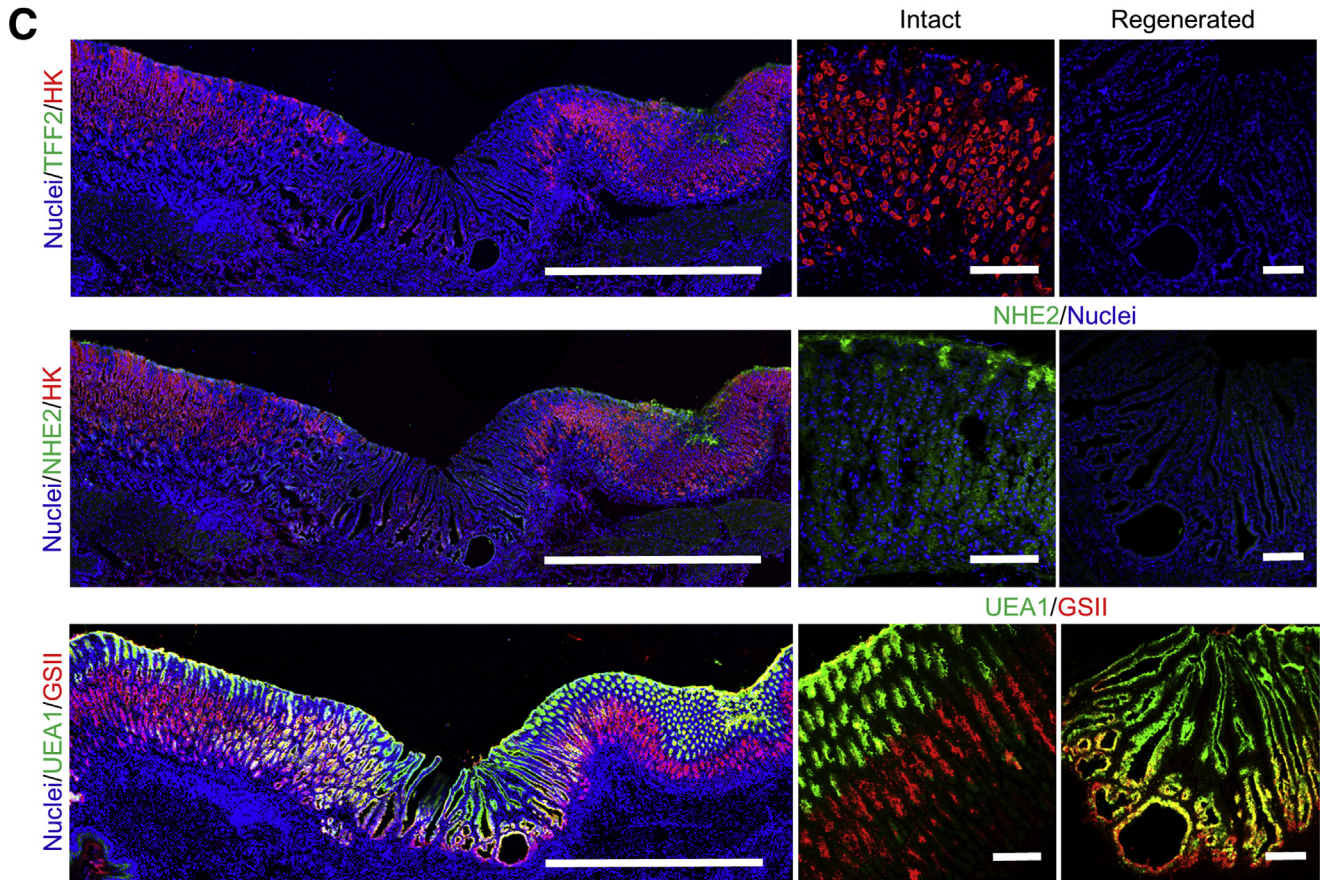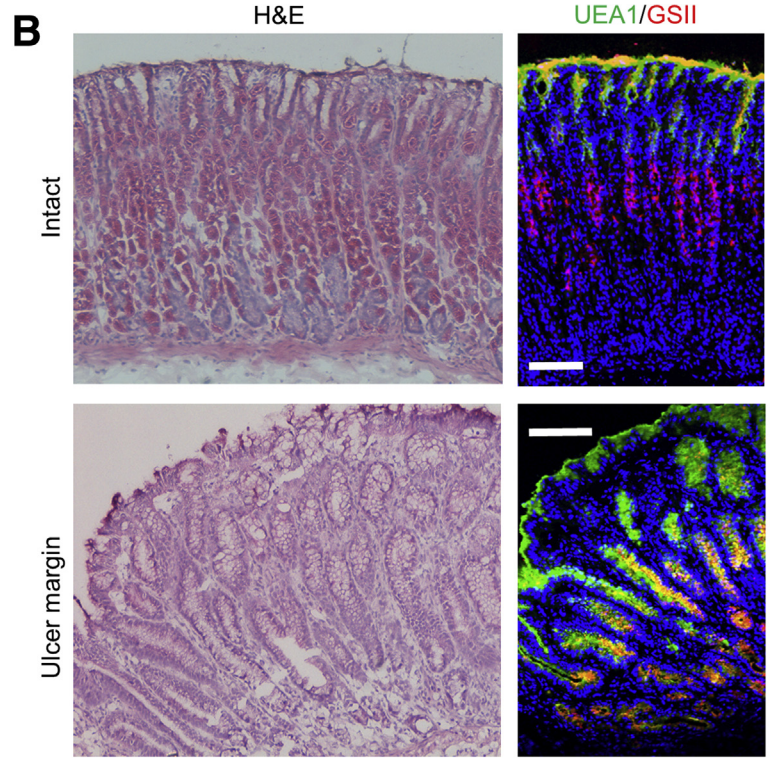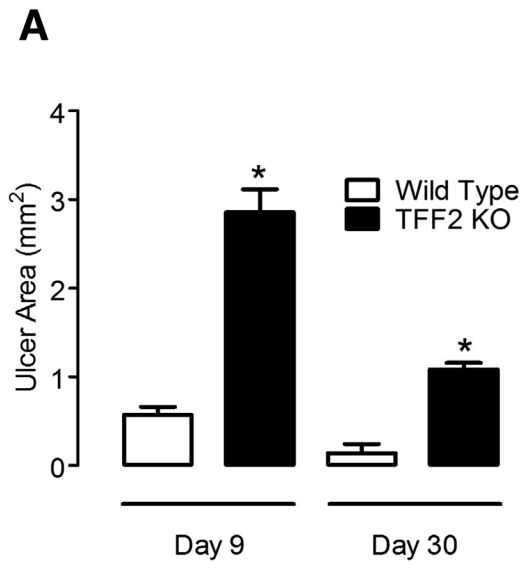
parietal cell markers, we observed significant up-regulation of a gastric atrophy marker,[30] gastrokine 3 (Gkn3). However, we did not observe any changes of caudal type homeobox (Cdx)1, Cdx2, or Muc2 expression, suggesting that intestinal metaplasia does not arise in the corpus ulcer healing process (Figure 3C).

Surface mucus marker ulex europaeus 1 (UEA-1) and neck mucus marker Griffonia simplicifolia lectin II (GSII) were expressed in their expected compartments of the gland in the intact epithelium (Figure 4A and B). However, both GSII and UEA-1–positive mucus staining also expanded into the bottom of the gland in the regenerated tissue (Figure 4A). GSII, which co-expresses with TFF2, is used as a marker of spasmolytic polypeptide expressing metaplasia (SPEM).[31–33] SPEM has been documented in the ulcerated area 7 days after ulceration induced by acetic acid.[12,31] Consistent with other findings at early time points after ulceration,[34] we confirmed that 30 days after ulceration TFF2 co-expressed with GSII in the deep gland of the regenerated epithelium (Figure 4B). The fold change values of DMP777/Helicobacter felis–induced SPEM-related genes, identified by RNAseq,[35] correlated positively to our RNAseq data, which showed borderline significance in DMP777 and nominal significance in H felis. Results confirmed that the day 30 ulcer regenerated epithelium included SPEM lineages. Interestingly, UEA-1 also was found in TFF2-expressing sites, whereas it was negative in the deepest gland where TFF2 and GSII were positive (Figure 4B). GIF and Bhlha15 (Basic Helix-Loop-Helix Family, Member A15, also known as Mist1) were down-regulated in the regenerated epithelium (Figure 3A–C). GIF was found at the base of the gland in the intact stomach (Figure 4C), but GIF-positive cells were down-regulated dramatically in the regenerated epithelium and were found only in the deepest gland where GSII is positive and UEA-1 is negative (Figure 4C). These data suggest that mature chief cells are not present in the regenerated epithelium.

Stem/Progenitor Zone in Regenerated Epithelium

Gastric epithelial proliferation normally occurs in the isthmus region where we observe Ki67-positive cells (Figure 5A). In contrast, Ki67-positive cells were found at the base of regenerated epithelium, and Ki67 immunoreactivity notably was localized in UEA-1– and GSII-positive cells (Figure 5A). We also observed that SOX9 was up-regulated in regenerated tissue (Figures 3A, B, D, and 5B), especially within UEA-1– and GSII-positive cells deep in the gland, whereas SOX9 expression was weak in the intact gastric epithelium and co-localized with GSII (Figure 5B). The expression pattern of SOX9 in regenerated epithelium appeared deeper in the gland than that of Ki67. Results

suggested that the stem/progenitor and proliferation zone both are present at the gland base of regenerated epithelium. In the RNAseq data, we found down-regulation of Tnfrsf19 (Tumor necrosis factor receptor superfamily, member 19, also known as Troy), Bmi1 (B lymphoma Mo-MLV insertion region 1 homolog), and Msi1 (Musashi RNA-binding protein 1), whereas we observed up-regulation of Prom1, SOX9, and SOX2 (Figure 3D). SOX2 was expressed in both nuclei and cytoplasmic compartments in the neck/isthmus of the mouse stomach (Figure 6), and was expressed sporadically in the entire epithelium, consistent with other findings.[21,36] SOX2-positive cells are partially positive for Ki67 or SOX9 in normal epithelium. Similarly, SOX2 was partially expressed in Ki67- and SOX9-positive cells in the regenerated epithelium. However, SOX2 expression was not strong in the base of the gland where SOX9 was up-regulated, although it was highly expressed in the earlier-described proliferation zone (Ki67) (Figure 6).

Because SOX9 also is expressed in the tuft cell, we checked the expression pattern of another tuft cell marker: DCLK1. It also has been reported that DCLK1-expressing cells are expanded in an ulcer,[12] as well as in response to loss of parietal cells.[37] We observed that DCLK1 was up-regulated significantly in the regenerated epithelium (Figures 3A–C and 5C). Immunofluorescence showed that DCLK1-positive cells also expressed SOX9, whereas a large number of SOX9-positive cells did not co-express with DCLK1 (Figure 5D). However, Ki67 was not expressed in DCLK1-positive cells (Figure 5E).

By using uninjured tissue, we also observed that GSII co-localized with Sox9 and Ki67 in the bottom of antral glands, and UEA-1–positive mucus was observed throughout the pyloric gland (Figure 7). We observed up-regulation of PDX1 in the regenerated epithelium, despite no expression of PDX1 in the normal corpus epithelium (Figures 3C and 8A). PDX1 was expressed in the antral epithelium (Figure 8B). However, gastrin (Figure 3C) or Lgr5 (Figure 3D) expression did not change in the corpus regenerated tissue and gastrin-positive cell was not detected in the regenerated epithelium (Figure 8C). These data suggest that regenerated corpus epithelium may share some antral features, but within the time frame evaluated there was no induction of mature antral cell types in the regenerated corpus epithelium under our experimental conditions.

Role of TFF2/NHE2 in Ulcer Healing

TFF2 is secreted predominantly by gastric neck cells and appears to have a central role in gastric injury and repair. TFFs promote gastric healing after injury through motogenic (cell migratory) and anti-apoptotic activities.[12,13,19,38]

Figure 9. (See previous page). **Gastric ulcer healing in TFF2 KO mouse.** (A) Gastric tissue was evaluated at 9 or 30 days after ulcer induction. Gastric ulcer size was measured and data are presented as means ± SEM (N = 6). *Significant difference at $P < .05$ vs WT. (B) Sections of gastric intact epithelium or ulcer margin in TFF2 KO at day 9. Images show H&E staining and UEA-1 (green), GSII (red) and nuclei (Hoechst33342: blue). Scale bar: 100 μm. (C) Sections of gastric regenerated epithelium in TFF2 KO at day 30 were dual-stained for H,K-ATPase (HK: red) and TFF2 (green) or NHE2 (green), and UEA-1 (green) and GSII (red). Left panel: low magnification (scale bar: 1 mm), right panel: high magnification (scale bar: 100 μm).
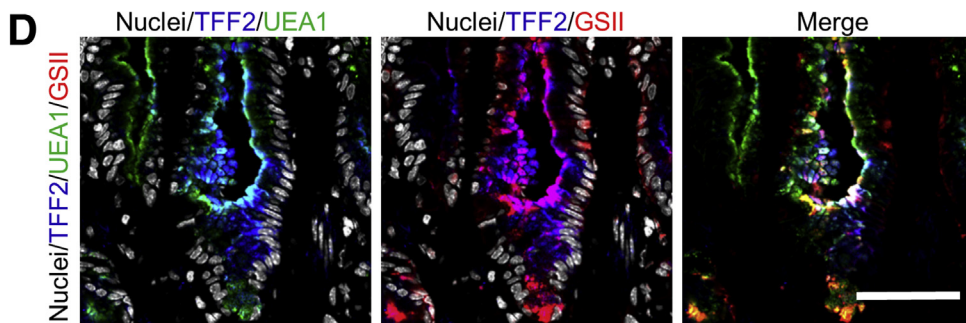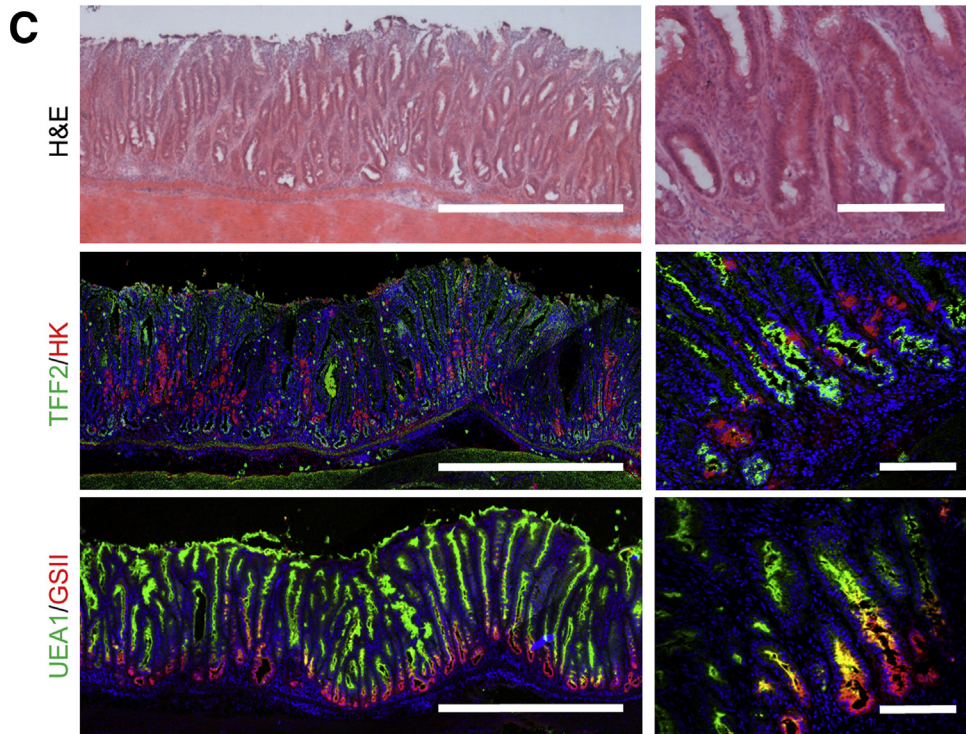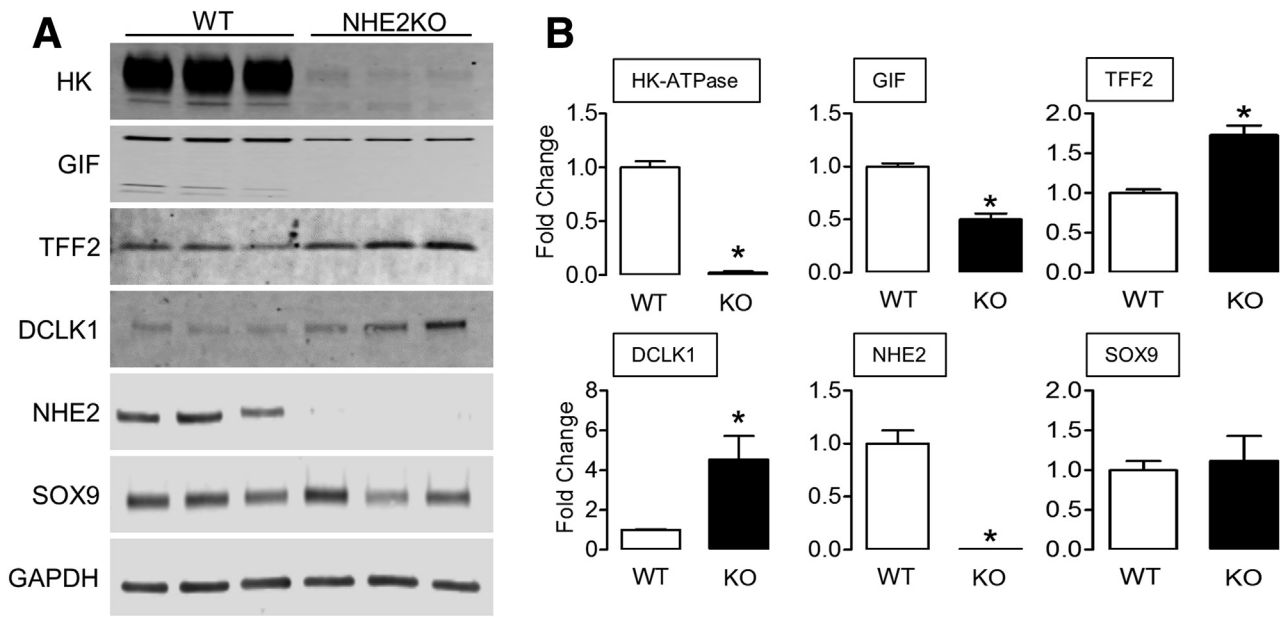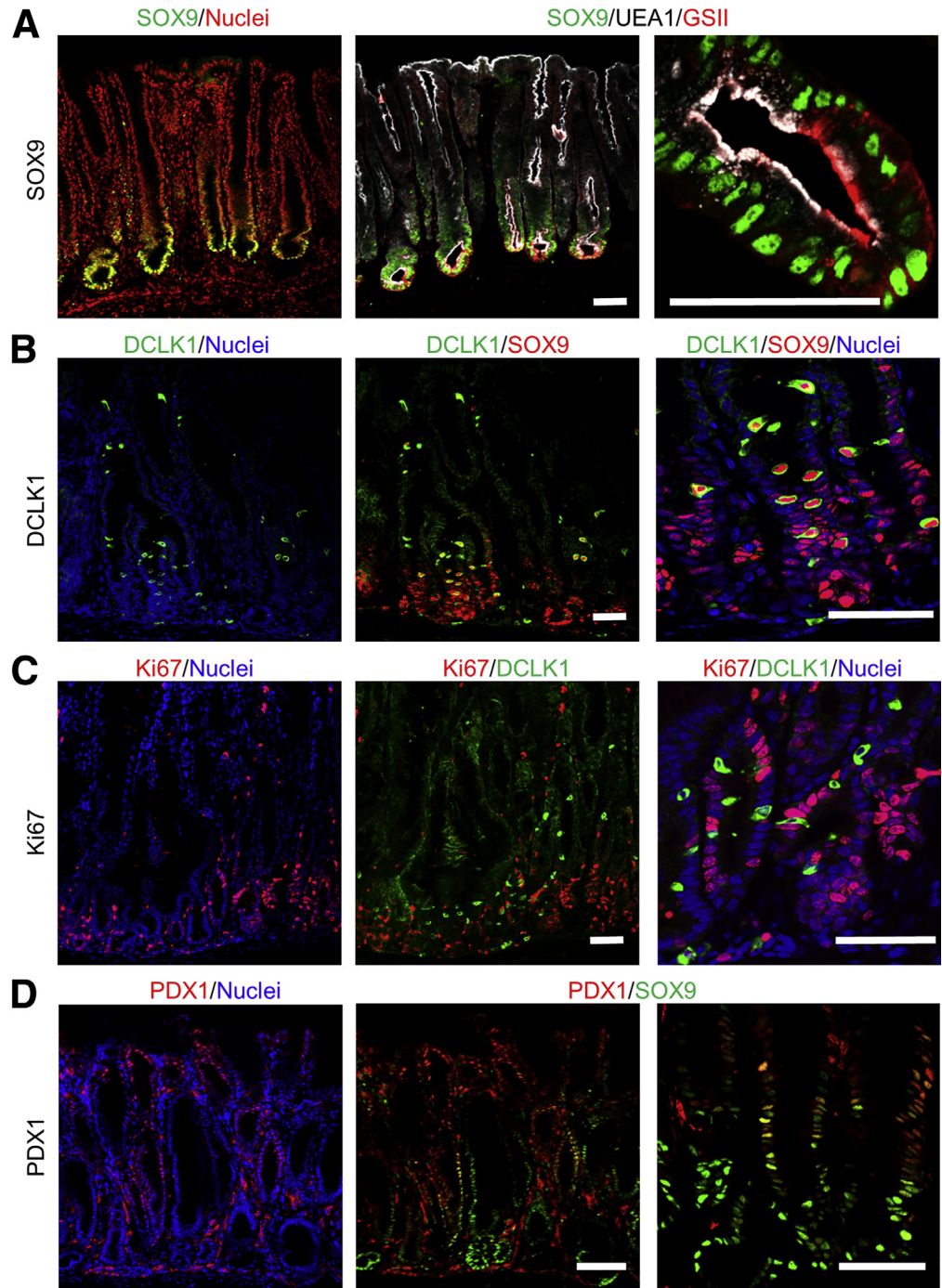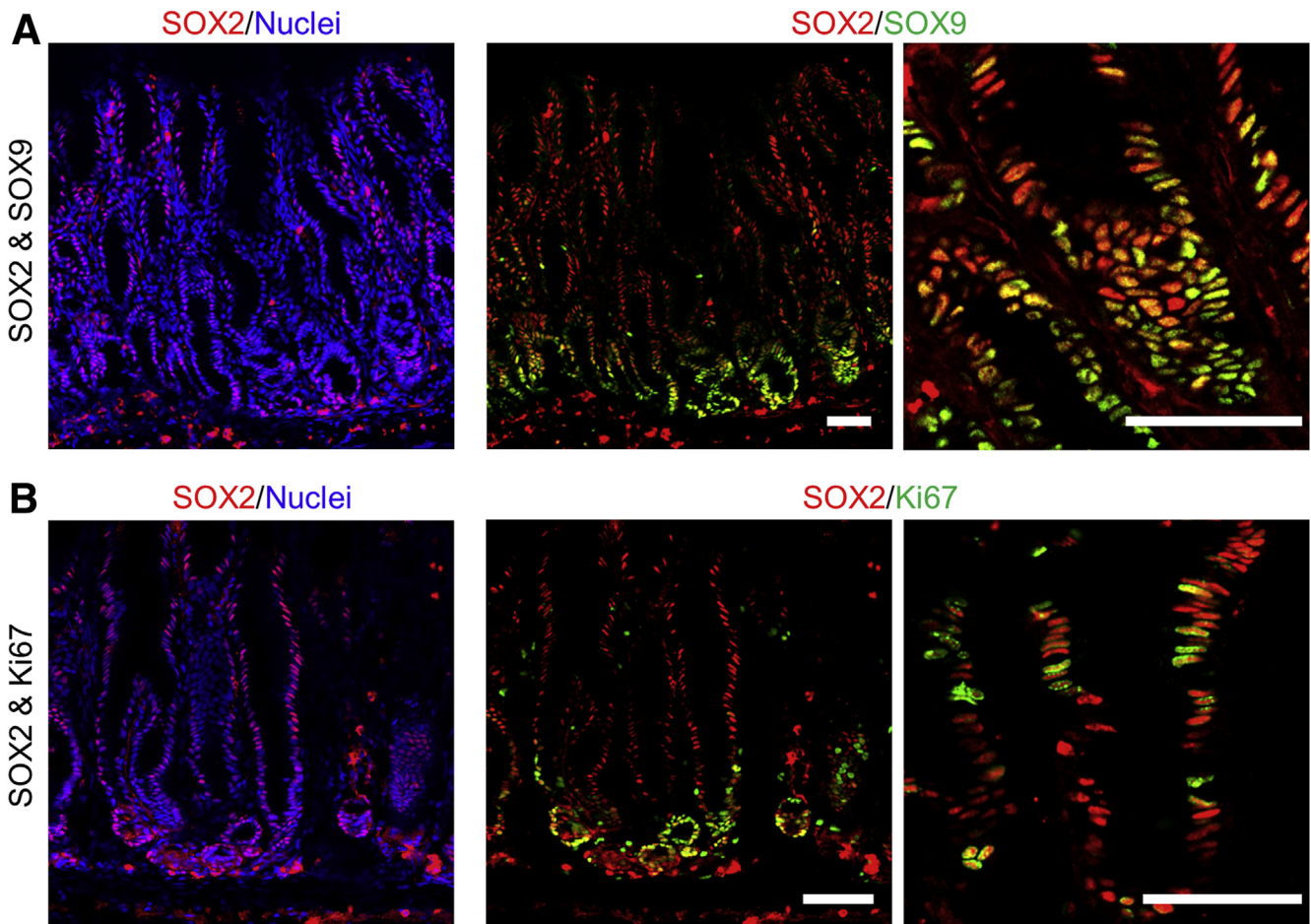
Figure 11. Gastric epithelium in NHE2 KO mouse. Immunofluorescence was performed in NHE2 KO mouse stomach. (*A*) Sections of NHE2 KO stomach were stained with SOX9 (*green*) and nuclei (Hoechst33342: *red*) or SOX9 (*red*), UEA-1 (*white*) and GSII (*red*). (*B*) DCLK1 (*green*), SOX9 (*red*), or (*C*) Ki67 (*red*), and (*D*) nuclei (*blue*), or PDX1 (*red*), SOX9 (*green*), and nuclei (*blue*). *Scale bars*: 50 μm.

We previously observed that TFF2 was up-regulated even at day 9 after ulceration,[11] and sustained an increase at day 30 (Figure 1). Although ulcer healing was delayed significantly in the TFF2 KO mouse stomach (Figure 9A), regeneration of the epithelium was observed at day 30 even in TFF2 KO mice, including sustained loss of HK-ATPase (Figure 9C). The expression pattern of UEA-1– and GSII-positive cells was similar to WT regenerated epithelium and we observed

---

Figure 10. (*See previous page*). Gastric epithelium in NHE2 KO mouse. Gastric tissue was obtained from WT and NHE2 KO mice. (*A*) Data show Western blot images of HK-ATPase (HK), TFF2, NHE2, SOX9, or GAPDH as indicated. (*B*) Compiled analysis of Western blots as in panel *A*, with results normalized to GAPDH. Results are presented as fold changes normalized to intact epithelium, means ± SEM (N = 4). *Significant difference at $P < .05$ vs WT. (*C*) Low- (*left panel*, *scale bar*: 1 mm) and high- (*right panel*, *scale bar*: 100 μm) magnification images of NHE2 KO mouse stomach, showing H&E, HK-ATPase (HK: *red*) and TFF2 (*green*), or UEA-1 (*green*) and GSII (*red*), respectively. (*D*) TFF2 (*blue*), UEA-1 (*green*), GSII (*red*), and nuclei (Hoechst33342: *white*) in NHE2 KO mouse stomach. *Scale bar*: 50 μm.

Figure 12. Expression of SOX2 in NHE2 KO mouse stomach. Immunofluorescence was performed in NHE2 KO mouse stomach. Sections of NHE2 KO stomach were stained with (*A*) SOX2 (*red*), SOX9 (*green*), or (*B*) Ki67 (*green*), and nuclei (Hoechst33342: *blue*). *Scale bars*: 50 μm.

mucous metaplasia both at day 9 and day 30 (Figure 9B and C). In addition, NHE2 was down-regulated in both intact and regenerated epithelium (Figure 9C), consistent with our previous observation that NHE2 expression was low in the TFF2 KO stomach.[16] These data suggest that TFF2 is involved most prominently in the initial closure of an ulcer, but only slows re-epithelialization.

TFF-dependent repair of (at least microscopic) gastric lesions requires the NHE2 Na/H exchanger isoform.[16] In normal tissue, we observed NHE2 expression in the surface epithelium and also in the deep gland, whereas we observed down-regulation of NHE2 in regenerated tissue (Figure 1E). Because we observed the down-regulation of NHE2 in regenerated epithelium, we considered the lack of NHE2 could contribute to TFF2 up-regulation or generation of the poor appearance of regenerated epithelium. To test this hypothesis, we compared some outcomes in the ulcer regenerated tissue with the healthy NHE2 KO stomach. In the NHE2 KO corpus, HK-ATPase and GIF protein was down-regulated significantly (Figure 10A and B), whereas TFF2 was up-regulated markedly deep in the gland and co-localized with GSII (Figure 10A–C). UEA-1–positive cells, also found deep in the gland, were co-localized with TFF2 or GSII

(Figure 10C and D). In addition, we found that DCLK1 was up-regulated significantly in NHE2 KO gastric epithelium, whereas there was no difference in SOX9 expression between WT and NHE2 KO stomach (Figure 10A and B). SOX9 was found deep in the gland as well as DCLK1-positive cells (Figure 11A and B). Ki67-positive cells also were observed deep in the gland, and did not overlap with DCLK1-positive cells (Figure 11C). Similar to ulcer regenerated epithelium, SOX2 was partially expressed in Ki67- and SOX9-positive cells in the NHE2 KO stomach throughout the entire epithelium (Figure 12A and B). On the other hand, we also observed that PDX1 was expressed throughout the NHE2 KO mouse corpus epithelium (Figure 11D). When combined, these results suggest that NHE2 has a role in the maintenance as well as construction of a normal gastric epithelium.

Long-Term Monitoring of Regenerated Epithelium

We monitored ulcer healing for up to 8 months to determine how long it takes to restore a normal gastric epithelium after an initial ulceration. In the same experimental series, we asked if the 30-day regenerated epithelium was differentially susceptible to subsequent damage. We inoculated low amounts of Sydney strain 1 *H pylori*

(10^6 per mouse in one inoculum) at 30 days after ulceration (Figure 13A). We visually observed that ulcer regenerated epithelium was disrupted by *H pylori* 14 days after inoculum (44 days after ulcer) (Figure 13B and C). It should be noted that no ulcer was observed in other sites of the stomach, suggesting that the regenerated epithelium defense is relatively weak. *H pylori* colonization in the ulcerated site was not consistently higher than that of uninjured sites (Figure 13D). The disruption of regenerated epithelium by *H pylori* did not heal by 8 months later (Figure 13B and C), although *H pylori* colonization in the stomach tended to decrease over time (Figure 13D).

At 44 days after ulceration without *H pylori*, HK-ATPase largely was lacking in regenerated epithelium. Then at 4 and 8 months after ulceration without *H pylori*, HK-ATPase expression began to return slowly, although *H pylori* significantly suppressed the return of HK-ATPase (Figure 13E). At 4 months, TFF2 and NHE2 sustained up-regulation and down-regulation in the regenerated epithelium, respectively (Figures 13E and 14), with TFF2 showing strong expression in the ulcerated site with *H pylori*. SOX9 was up-regulated significantly in regenerated epithelium with and without *H pylori* (Figure 13E). SOX9, Ki67, GSII, and UEA-1 expression patterns were similar to those in the day 30 regenerated epithelium (Figure 14). However, distribution of SOX9 and Ki67 was similar to non–*H pylori* conditions (Figure 14).

At 8 months after ulceration without *H pylori*, we clearly observed HK-ATPase and NHE2 expression in the regenerated epithelium and a decrease of TFF2 in the bottom of the gland (Figures 13E and 15). Furthermore UEA-1, GSII, Ki67, and SOX9 expression patterns became more similar to normal gastric epithelium, although the height of epithelium still was shorter (Figure 15). Conversely, no recovery of HK-ATPase and NHE2 was found in the relapsed ulcer site caused by *H pylori*, and TFF2 expression remained high (Figure 13E). In addition, we observed a strong up-regulation of Ki67 distribution and SOX9 in the ulcerated site as well as intact area (Figure 15), suggesting that *H pylori* also affects the intact area at this late time point. However, only in the ulcerated area was UEA-1 co-localized with GSII. These results suggest that ulcer regenerated epithelium takes more than 8 months to return to normal, and has the potential to progress to further damage, with further insulting injury to the gastric mucosa.

Discussion

We have shown using a mouse model that ulcer regenerated epithelium is characterized by abnormal epithelium that is sustained for almost half a lifetime. Furthermore, repaired tissues are more susceptible to subsequent damage. Consistent with this, in human beings, long-term follow-up studies (up to 17 years) have shown that gastric recurrence or cancer development still is observed in many ulcer patients, even with successful *H pylori* eradication.[5] The gastric mucosa is exposed to acid and other chemical hazards, including food intake, assuming that there is a high chance to receive several challenges during ulcer healing. In the acetic acid–induced ulcer rodent model, several reports have shown that administration of nonsteroidal anti-inflammatory drugs or *H pylori* causes an ulcer in the area where the initial ulcer had healed,[10,39,40] although why an offense-induced relapse ulcer occurs at the same site or near the site still is unknown. In the present study, we observed that *H pylori* causes ulcer relapse, specifically at the site of visually healed regenerated epithelium. In addition, *H pylori*–infected regenerated epithelium sustains metaplasia and morphologic abnormalities. The low inoculum of *H pylori* that we used in the present study explains why it was unable to generate inflammation in the intact gastric epithelium, and our work suggests that the regenerated epithelium has weakened defenses against *H pylori*.

We found that metaplasia occurs in the regenerated epithelium and the metaplastic state is sustained for at least 4 months during normal ulcer healing. Previous studies have shown that a loss of parietal cells induces metaplasia in the stomach.[12,19,24,38] It has been reported that DCLK1 is up-regulated in response to a loss of parietal cells and metaplasia, including ulcerated tissue, but its functional role remains unknown.[12,37] Because DCLK1-positive cells were not positive for Ki67, they likely do not function as stem/progenitor cells. In the ulcer, UEA-1–positive cells expanded deep into the gland along with GSII- or TFF2-positive cells. Maloum et al[41] also observed an increase in the number of UEA-1–positive cells that were found deep in the gland, along with mucous metaplasia, a loss of parietal cells, and down-regulation of MUC5ac. UEA-1 binds α-L-fucose–containing glycoproteins. It has been reported that some human TFF2 contains unusual fucosylated oligosaccharide,[42] but we observed UEA-1 staining deep in the gland of regenerated epithelium in TFF2 KO mice. Fucosylation is involved in many physiological and pathologic processes such as development, cell proliferation, and inflammation.[43] We observed an increase in the number of UEA-1–positive cells, but it is unclear if this expansion of staining simply is owing to more cells of a defined type, such as gastric foveolar hyperplasia, or an expansion of fucosylation among a diverse set of cell types.

We reported that TFF2 plays an important role in gastric epithelial restitution through CXCR4 in response to microscopic damage.[16,44] The surface epithelial/metastasis markers TFF2 and CXCR4 are up-regulated and the former is confirmed to be widely distributed deep in the regenerated gastric gland. It also has been reported that CXCR4 is up-regulated at the ulcer granulation tissue and this expression is inhibited by acetylacetic acid administration, resulting in delayed ulcer healing.[45] In the present study, we showed that ulcer healing was delayed in the TFF2 KO mouse stomach, although we observed regenerated epithelium. This suggests that TFF2 may be involved in the regulation of proliferation as well. It also has been reported that TFF2 contributes to proliferation.[46] On the other hand, it has been reported that *H pylori* accelerates the progression of gastritis to dysplasia (6 months) in the TFF2 KO mouse stomach, although the development of atrophy and epithelial hyperplasia appeared 19 month after *H pylori* inoculation in the wild-type mouse stomach.[47] We observed that TFF2 is
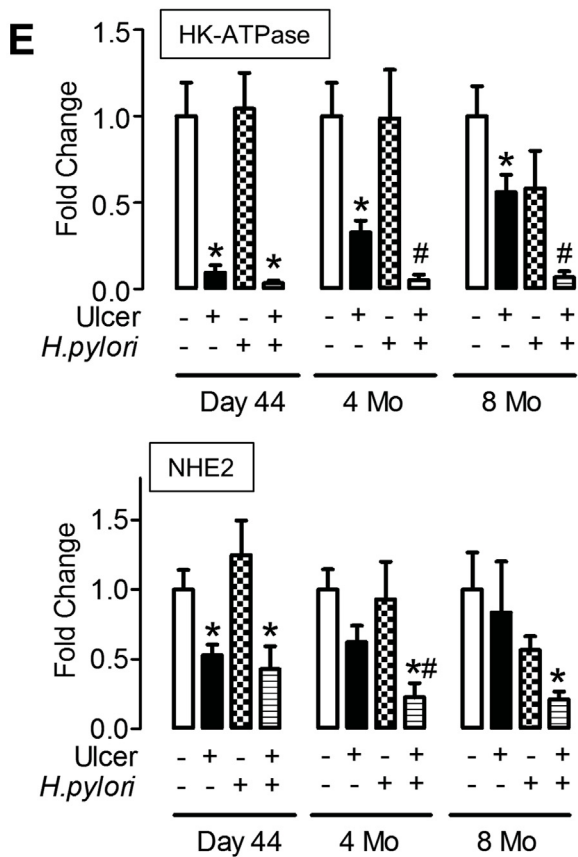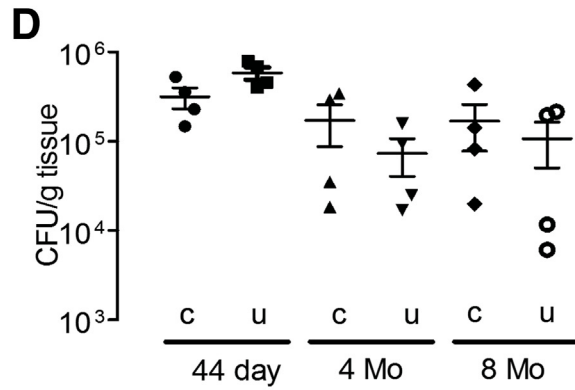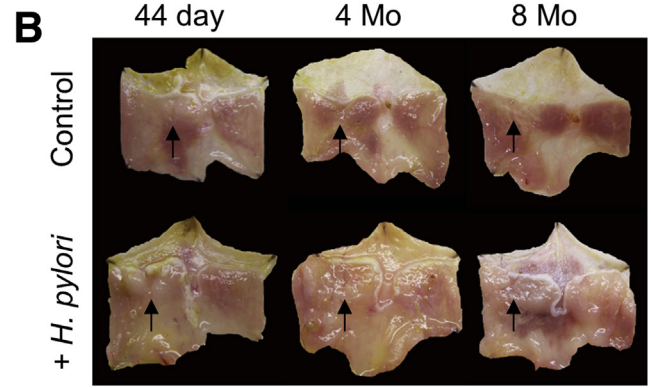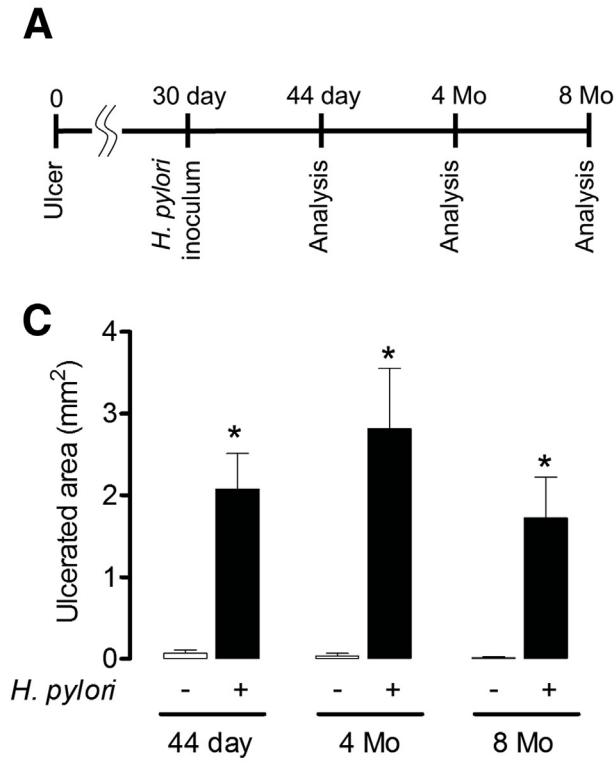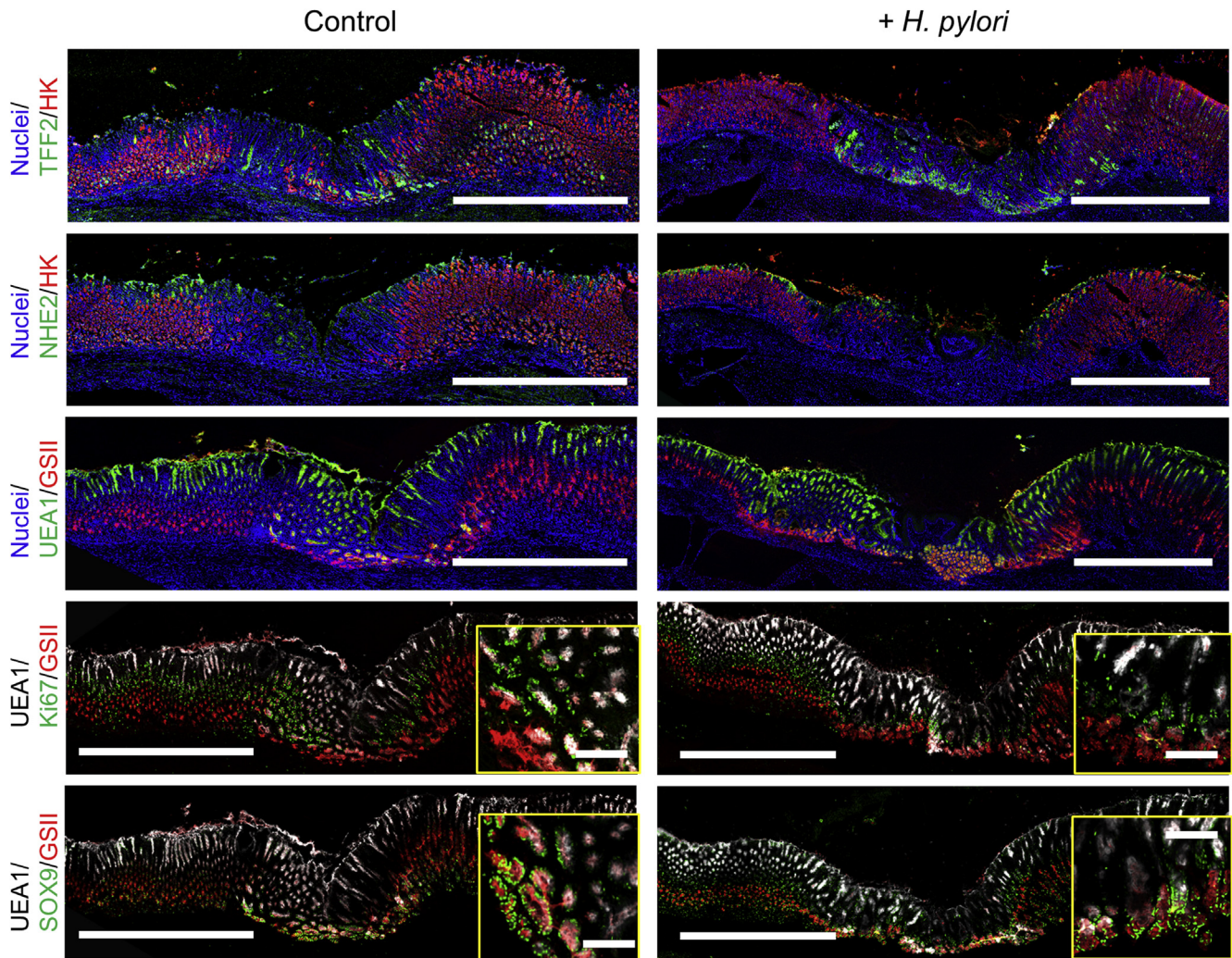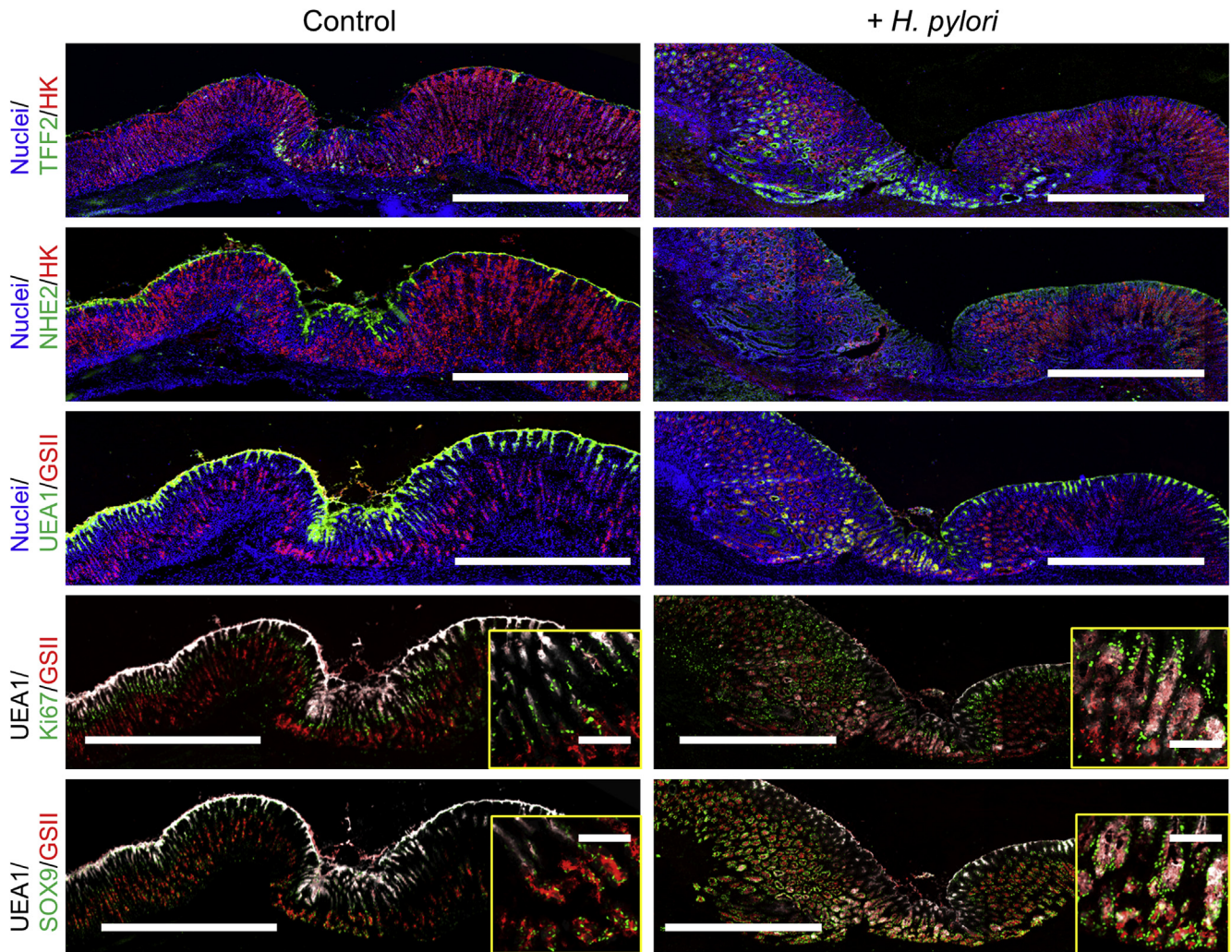
Figure 14. Morphology of gastric regenerated epithelium at 4 months after ulceration. Gastric ulcer was induced by topical serosal application of acetic acid. In some animals, a single gavage of 10^6 *H pylori* was performed 30 days after ulcer induction. Results are compared from the same tissue and sectioning series, although adjacent sections are not always presented. Sections of uninfected (control) or *H pylori*–infected tissues are used. Images show dual staining for HK-ATPase (HK: *red*) and TFF2 (*green*), HK-ATPase (HK: *red*) and NHE2 (*green*), or UEA-1 (*green*) and GSII (*red*), and triple staining for Ki67 or SOX9 (*green*) with UEA-1 (*white*) and GSII (*red*). *Scale bar*: 1 mm. For Ki67 and SOX9, high-magnification images of regenerated epithelium are shown in the *yellow box*. *Scale bar*: 100 μm.

up-regulated in the ulcerated area in *H pylori* infection even 8 months after an ulcer episode. Furthermore, it has been reported that TFF2 acts as a tumor suppressor in gastric carcinogenesis and TFF2 mRNA and protein are down-regulated in gastric adenomas,[13,48,49] these results suggest that up-regulation of TFF2 contributes to prevent cancer progression in the ulcer regenerated gastric epithelium. We did not detect any cancer-like morphology even 8 month after ulceration in the wild-type mouse stomach. Thus, up-regulation of TFF2 is likely a necessary event in regenerated or inflamed tissue, which could prevent further developing pathologic changes in the long term.

Figure 13. (*See previous page*). **Gastric regenerated epithelium at long-term period, and ulcer relapse by H pylori.** (*A*) Schematic of experimental timeline. A single gavage of 10^6 *H pylori* was performed 30 days after ulcer induction. Gastric ulcer was evaluated at 14 days (44 days after ulceration), 3 months (4 months after ulceration), or 7 months (8 months after ulceration) after *H pylori* inoculation. (*B*) Gross morphology at each experimental time point after inoculation with 10^6 *H pylori*. Control tissue was from mice uninfected with *H pylori*. (*C*) Gastric ulcer size was measured and data are presented as means ± SEM (N = 5–7). *Significant difference at $P < .05$ vs negative *H pylori*. (*D*) Harvested ulcer regenerated (u) or nonulcerated control (c) gastric tissue was collected from the same mouse, homogenized, and *H pylori* was cultured on Columbia blood agar plates to obtain colony-forming units (CFU). Data are presented as CFU/g tissue (N = 4). No CFU was detected in mice not infected with *H pylori*. (*E*) HK-ATPase, TFF2, NHE2, or SOX9 mRNA was detected by real-time PCR. Data are shown as fold change normalized to the nonulcerated region of the uninfected group (ulcer -, *H pylori* -). Means ± SEM (N = 5–7). *$P < .05$ vs intact region (ulcer -, *H pylori* -). #$P < .05$ vs ulcer region in no *H pylori* inoculation group (ulcer +, *H pylori* -).

Figure 15. Morphology of gastric regenerated epithelium at 8 months after ulceration. Gastric tissue was isolated 8 month after ulcer induction. Results are compared from the same tissue and sectioning series, although adjacent sections are not always presented. Sections of uninfected (control) or *H pylori*–infected tissues are used. Images show dual staining for HK-ATPase (HK: *red*) and TFF2 (*green*), HK-ATPase (HK: *red*) and NHE2 (*green*), or UEA-1 (*green*) and GSII (*red*), and triple staining for Ki67 or SOX9 (*green*) with UEA-1 (*white*) and GSII (*red*). Scale bar: 1 mm. For Ki67 and SOX9, high-magnification images of regenerated epithelium are shown in the *yellow* box. Scale bar: 100 μm.

We previously reported that NHE2 plays a novel (albeit unknown) role as an effector of TFF2 in gastric surface epithelial restitution.[16] We observed the down-regulation of NHE2 in the regenerated epithelium where TFF2 is up-regulated. This suggests that the regenerated epithelium has a weakened defense against insult, which may explain why a low abundance of *H pylori* selectively could relapse the ulcer at the site of the regenerated tissue. In the present study, we observed that the number of parietal cells are decreased in NHE2 KO corpus. This is consistent with another finding that NHE2 KO stomachs have fewer parietal cells with hyperplasia/atrophy.[15] The same group also suggested that NHE2 is essential for parietal cell long-term viability.[50] It is likely that NHE2 deletion leads to a loss of parietal cells, resulting in the generation of abnormal epithelium, which is similar to ulcer-induced regenerated epithelium. Although NHE2 may be involved in cell differentiation, further investigation will be needed to determine whether NHE2 affects the local ionic environment or directly alters the cell differentiation pathway through another mechanism.

Stem cells in the gastric corpus epithelium have not been fully identified yet, although proliferating cells normally are detected in the isthmus. We observed strong proliferation activity in the base of regenerated epithelium where the UEA-1, GSII, and TFF2 abnormally is expressed at 30 days after ulceration. In addition, SOX9 was up-regulated in the same region, and returned to normal expression levels during long-term ulcer healing. We also observed that SOX2, which recently was reported as a gastric corpus stem cell marker,[21] was up-regulated in the regenerated epithelium, although it does not specifically appear in the proliferative (Ki67+) compartment. SOX9 reportedly is up-regulated within mucous metaplasia or gastric carcinoma.[22–24] Gupta et al[22] reported that up-regulated SOX9 co-expressed with

GSII, and some SOX9-positive cells showed proliferating activity. Although SOX9 marks tuft cells and mucous metaplasia in our current experiments, some SOX9-positive cells also may be stem/progenitors to regenerate tissue in response to injury. This could be resolved only using SOX9 lineage tracing experiments in the regenerated epithelium. Lgr5+ cells now are recognized as the stem cell in antrum, small intestine, and colon,[17] but the expression of Lgr5 in the adult corpus is limited. We did not see any changes of Lgr5 mRNA in the regenerated tissue. It is reported that Lgr5+ cells are not involved in developing metaplasia in mouse corpus.[19] Thus, Lgr5+ cells are unlikely to play any role in ulcer regeneration in the corpus. More recently, *Troy*-positive cells were expressed at the corpus gland base in a subset of differentiated chief cells and showed that sorted *Troy*-positive chief cells generate long-lived gastric organoids, and these cultures were differentiated toward the mucus-producing cell lineages of the neck and pit regions.[12,20] *Troy* has been proposed as a marker of quiescent stem-like cells, but *Troy* mRNA did not change in the regenerated epithelium. However, it is possible that Lgr5+ cells or *Troy*-positive cells give rise to progenitor cells, although they do not renew themselves. Further studies will be needed to identify the stem cells that respond to regenerate the damaged gastric epithelium.

A central question is whether such outcomes occur in human beings. In human beings there is some limited evidence that there is a longer time for recovery of parietal cells after injury. Blom[51] showed that parietal cells did not reappear until 3 months after ulcer repair, and even by 8–9 months the number of parietal cells in the regenerated gastric mucosa never reached normal levels. We observed that PDX1 was increased in the regenerated epithelium. Although regenerated epithelium may have features of antral epithelium based on the expression patterns of mucus, SOX9, and PDX1, we did not detect any genes of mature antral cell types, such as gastrin. Other investigators also found PDX1 expression in the adjacent gastric gland in atrophic corpus gastritis.[52] They suggested that PDX1 may play a role in the initiation of metaplasia.[52] It also has been reported that overexpression of transforming growth factor-α stimulated PDX1 throughout corpus atrophic epithelium with up-regulation of TFF2 in the deep gland.[53] Importantly, they found that inhibition of PDX1 by anti–epidermal growth factor antibody led to an increase in the number of parietal cells.[53] More recently, the same group found that inhibition of mitogen-activated protein kinase (downstream of epidermal growth factor-receptor signaling) regresses metaplasia in the stomach and turned on the normal gastric gland lineage, including the appearance of parietal cells.[54] Our RNAseq analyses showed that transforming growth factor-α and epidermal growth factor receptor were up-regulated in the regenerated epithelium. Thus, these findings could provide an explanation of why differentiation to parietal cells was slow in the regenerated epithelium in our ulcer model. Further studies will be needed to investigate this point.

We conclude that even after visual evidence of healing from gastric ulceration, it cannot be assumed that the tissue is normal. The gene expression profile and morphology of the regenerated epithelium is abnormal in mice for the long term, and this can contribute to further damage. This is especially important because the gastric epithelium is exposed continually to harsh environments and is exposed commonly to the pathogen *H pylori*. In human patients, the ulcer recurrence rate is varied among the studies as well as countries, but overall there is a concurrence regarding the beneficial effect of *H pylori* eradication or anti-ulcer medicine on ulcer recurrence. Laine et al[55] observed a 20% ulcer recurrence rate at 6 months in patients with successful *H pylori* eradication and nonsteroidal anti-inflammatory drug users. They also reported that the ulcer recurrence rate was increased over time (ie, 6 months, 0%; 12 months, 7.5%; 18 months, 10%; and 24 months, 10%) in patients in whom *H pylori* was eradicated.[56] We speculate that the regenerated epithelium in patients may be molecularly and cellularly abnormal for years, and that this increases the risk for a variety of gastric disorders. Further study is needed in human patients because it may be necessary to develop a more rigorous diagnostic criterion for ulcer healing as an opportunity to protect against prevention of further damage.

References

1. Okabe S, Amagase K. An overview of acetic acid ulcer models–the history and state of the art of peptic ulcer research. Biol Pharm Bull 2005;28:1321–1341.
2. Wallace JL. Prostaglandins, NSAIDs, and gastric mucosal protection: why doesn't the stomach digest itself? Physiol Rev 2008;88:1547–1565.
3. Tarnawski A, Stachura J, Krause WJ, et al. Quality of gastric ulcer healing: a new, emerging concept. J Clin Gastroenterol 1991;13(Suppl 1):S42–S47.
4. Take S, Mizuno M, Ishiki K, et al. The effect of eradicating Helicobacter pylori on the development of gastric cancer in patients with peptic ulcer disease. Am J Gastroenterol 2005;100:1037–1042.
5. Take S, Mizuno M, Ishiki K, et al. Seventeen-year effects of eradicating Helicobacter pylori on the prevention of gastric cancer in patients with peptic ulcer; a prospective cohort study. J Gastroenterol 2015;50:638–644.
6. Molloy RM, Sonnenberg A. Relation between gastric cancer and previous peptic ulcer disease. Gut 1997; 40:247–252.
7. Hong JB, Zuo W, Wang AJ, et al. Gastric ulcer patients are more susceptible to developing gastric cancer compared with concomitant gastric and duodenal ulcer patients. Oncol Lett 2014;8:2790–2794.
8. Mitsunaga A, Tagata T, Hamano T, et al. Metachronous early gastric cancer over a period of 13 years after eradication of Helicobacter pylori. Clin J Gastroenterol 2014;7:490–495.
9. Fuccio L, Zagari RM, Eusebi LH, et al. Meta-analysis: can Helicobacter pylori eradication treatment reduce the risk for gastric cancer? Ann Intern Med 2009;151:121–128.
10. Young Oh T, Ok Ahn B, Jung Jang E, et al. Accelerated ulcer healing and resistance to ulcer recurrence with

gastroprotectants in rat model of acetic acid-induced gastric ulcer. J Clin Biochem Nutr 2008;42:204–214.

11. Aihara E, Closson C, Matthis AL, et al. Motility and chemotaxis mediate the preferential colonization of gastric injury sites by Helicobacter pylori. PLoS Pathog 2014;10:e1004275.

12. Kikuchi M, Nagata H, Watanabe N, et al. Altered expression of a putative progenitor cell marker DCAMKL1 in the rat gastric mucosa in regeneration, metaplasia and dysplasia. BMC Gastroenterol 2010;10:65.

13. Weis VG, Petersen CP, Mills JC, et al. Establishment of novel in vitro mouse chief cell and SPEM cultures identifies MAL2 as a marker of metaplasia in the stomach. Am J Physiol Gastrointest Liver Physiol 2014;307:G777–G792.

14. Petersen CP, Weis VG, Nam KT, et al. Macrophages promote progression of spasmolytic polypeptide-expressing metaplasia after acute loss of parietal cells. Gastroenterology 2014;146:1727–1738 e8.

15. Boivin GP, Schultheis PJ, Shull GE, et al. Variant form of diffuse corporal gastritis in NHE2 knockout mice. Comp Med 2000;50:511–515.

16. Xue L, Aihara E, Wang TC, et al. Trefoil factor 2 requires Na/H exchanger 2 activity to enhance mouse gastric epithelial repair. J Biol Chem 2011; 286:38375–38382.

17. Mahe MM, Aihara E, Schumacher MA, et al. Establishment of gastrointestinal epithelial organoids. Curr Protoc Mouse Biol 2013;3:217–240.

18. Barker N, Huch M, Kujala P, et al. Lgr5(+ve) stem cells drive self-renewal in the stomach and build long-lived gastric units in vitro. Cell Stem Cell 2010;6:25–36.

19. Nam KT, O'Neal RL, Coffey RJ, et al. Spasmolytic polypeptide-expressing metaplasia (SPEM) in the gastric oxyntic mucosa does not arise from Lgr5-expressing cells. Gut 2012;61:1678–1685.

20. Stange DE, Koo BK, Huch M, et al. Differentiated Troy+ chief cells act as reserve stem cells to generate all lineages of the stomach epithelium. Cell 2013;155:357–368.

21. Arnold K, Sarkar A, Yram MA, et al. Sox2(+) adult stem and progenitor cells are important for tissue regeneration and survival of mice. Cell Stem Cell 2011;9:317–329.

22. Gupta A, Wodziak D, Tun M, et al. Loss of anterior gradient 2 (Agr2) expression results in hyperplasia and defective lineage maturation in the murine stomach. J Biol Chem 2013;288:4321–4333.

23. Sashikawa Kimura M, Mutoh H, Sugano K. SOX9 is expressed in normal stomach, intestinal metaplasia, and gastric carcinoma in humans. J Gastroenterol 2011; 46:1292–1299.

24. Mills JC, Sansom OJ. Reserve stem cells: differentiated cells reprogram to fuel repair, metaplasia, and neoplasia in the adult gastrointestinal tract. Sci Signal 2015;8:re8.

25. Rosenbloom KR, Armstrong J, Barber GP, et al. The UCSC Genome Browser database: 2015 update. Nucleic Acids Res 2015;43:D670–D681.

26. Chen J, Bardes EE, Aronow BJ, et al. ToppGene Suite for gene list enrichment analysis and candidate gene prioritization. Nucleic Acids Research 2009;37:W305-311.

27. Kaimal V, Bardes EE, Tabar SC, et al. ToppCluster: a multiple gene list feature analyzer for comparative enrichment clustering and network-based dissection of biological systems. Nucleic Acids Research 2010;38: W96-102.

28. Shannon P, Markiel A, Ozier O, et al. Cytoscape: a software environment for integrated models of biomolecular interaction networks. Genome Research 2003; 13:2498–2504.

29. Dubeykovskaya Z, Dubeykovskiy A, Solal-Cohen J, et al. Secreted trefoil factor 2 activates the CXCR4 receptor in epithelial and lymphocytic cancer cell lines. J Biol Chem 2009;284:3650–3662.

30. Menheniott TR, Peterson AJ, O'Connor L, et al. A novel gastrokine, Gkn3, marks gastric atrophy and shows evidence of adaptive gene loss in humans. Gastroenterology 2010;138:1823–1835.

31. Nozaki K, Ogawa M, Williams JA, et al. A molecular signature of gastric metaplasia arising in response to acute parietal cell loss. Gastroenterology 2008; 134:511–522.

32. Ogawa M, Nomura S, Varro A, et al. Altered metaplastic response of waved-2 EGF receptor mutant mice to acute oxyntic atrophy. Am J Physiol Gastrointest Liver Physiol 2006;290:G793–G804.

33. Kang W, Rathinavelu S, Samuelson LC, et al. Interferon gamma induction of gastric mucous neck cell hypertrophy. Lab Invest 2005;85:702–715.

34. Engevik A, Feng R, Li J, et al. Transplantation of gastric organoid-derived spasmolytic polypeptide/TFF2-expressing metaplasia (SPEM) cell lineage promotes ulcer repair in the aged stomach. FASEB J 2015; 29(Supplement):849.4.

35. Weis VG, Sousa JF, LaFleur BJ, et al. Heterogeneity in mouse spasmolytic polypeptide-expressing metaplasia lineages identifies markers of metaplastic progression. Gut 2013;62:1270–1279.

36. Asonuma S, Imatani A, Asano N, et al. Helicobacter pylori induces gastric mucosal intestinal metaplasia through the inhibition of interleukin-4-mediated HMG box protein Sox2 expression. Am J Physiol Gastrointest Liver Physiol 2009;297:G312–G322.

37. Choi E, Petersen CP, Lapierre LA, et al. Dynamic expansion of gastric mucosal doublecortin-like kinase 1-expressing cells in response to parietal cell loss is regulated by gastrin. Am J Pathol 2015;185: 2219–2231.

38. Nomura S, Baxter T, Yamaguchi H, et al. Spasmolytic polypeptide expressing metaplasia to preneoplasia in H. felis-infected mice. Gastroenterology 2004;127:582–594.

39. Keto Y, Ebata M, Tomita K, et al. Influence of Helicobacter pylori infection on healing and relapse of acetic acid ulcers in Mongolian gerbils. Dig Dis Sci 2002; 47:837–849.

40. Wang GZ, Huang GP, Yin GL, et al. Aspirin can elicit the recurrence of gastric ulcer induced with acetic acid in rats. Cell Physiol Biochem 2007;20:205–212.

41. Maloum F, Allaire JM, Gagne-Sansfacon J, et al. Epithelial BMP signaling is required for proper specification of epithelial cell lineages and gastric endocrine cells. Am J Physiol Gastrointest liver Physiol 2011; 300:G1065–G1079.

42. Hanisch FG, Ragge H, Kalinski T, et al. Human gastric TFF2 peptide contains an N-linked fucosylated N,N'-diacetyllactosediamine (LacdiNAc) oligosaccharide. Glycobiology 2013;23:2–11.

43. Ma B, Simala-Grant JL, Taylor DE. Fucosylation in prokaryotes and eukaryotes. Glycobiology 2006; 16:158R–184R.

44. Xue L, Aihara E, Podolsky DK, et al. In vivo action of trefoil factor 2 (TFF2) to speed gastric repair is independent of cyclooxygenase. Gut 2010;59:1184–1191.

45. Sato T, Amano H, Ito Y, et al. NSAID, aspirin delays gastric ulcer healing with reduced accumulation of CXCR4(+)VEGFR1(+) cells to the ulcer granulation tissues. Biomed Pharmacother 2013;67:607–613.

46. Farrell JJ, Taupin D, Koh TJ, et al. TFF2/SP-deficient mice show decreased gastric proliferation, increased acid secretion, and increased susceptibility to NSAID injury. J Clin Invest 2002;109:193–204.

47. Fox JG, Rogers AB, Whary MT, et al. Accelerated progression of gastritis to dysplasia in the pyloric antrum of TFF2 -/- C57BL6 x Sv129 Helicobacter pylori-infected mice. Am J Pathol 2007;171: 1520–1528.

48. Jiang P, Yu G, Zhang Y, et al. Promoter hypermethylation and downregulation of trefoil factor 2 in human gastric cancer. Oncol Lett 2014;7:1525–1531.

49. Kim H, Eun JW, Lee H, et al. Gene expression changes in patient-matched gastric normal mucosa, adenomas, and carcinomas. Exp Mol Pathol 2011;90:201–209.

50. Schultheis PJ, Clarke LL, Meneton P, et al. Targeted disruption of the murine Na+/H+ exchanger isoform 2 gene causes reduced viability of gastric parietal cells and loss of net acid secretion. J Clin Invest 1998; 101:1243–1253.

51. Blom H. The structure of normal and regenerating rat oxyntic mucosa. Scand J Gastroenterol Suppl 1985; 110:73–80.

52. Buettner M, Dimmler A, Magener A, et al. Gastric PDX-1 expression in pancreatic metaplasia and endocrine cell hyperplasia in atrophic corpus gastritis. Mod Pathol 2004;17:56–61.

53. Nomura S, Settle SH, Leys CM, et al. Evidence for repatterning of the gastric fundic epithelium associated with Menetrier's disease and TGFalpha overexpression. Gastroenterology 2005;128:1292–1305.

54. Choi E, Hendley AM, Bailey JM, et al. Expression of activated Ras in gastric chief cells of mice leads to the full spectrum of metaplastic lineage transitions. Gastroenterology 2016;150:918–930.

55. Laine L, Hopkins RJ, Girardi LS. Has the impact of Helicobacter pylori therapy on ulcer recurrence in the United States been overstated? A meta-analysis of rigorously designed trials. Am J Gastroenterol 1998;93:1409–1415.

56. Kim N, Oh JH, Lee CG, et al. Effect of eradication of Helicobacter pylori on the benign gastric ulcer recurrence–a 24 month follow-up study. Korean J Intern Med 1999;14:9–14.